HUMANOID ROBOT LEG AND ARM COORDINATION FOR FORCE CONTROL APPLICATIONS

by
BUĞRA SARAÇ

Submitted to the Graduate School of Engineering and Natural Sciences
in partial fulfilment of
the requirements for the degree of Master of Science

Sabancı University
July 2024

ABSTRACT

HUMANOID ROBOT LEG AND ARM COORDINATION FOR FORCE CONTROL APPLICATIONS

BUĞRA SARAÇ

MECHATRONICS ENGINEERING M.A. THESIS, JULY 2024

Thesis Supervisor: Associate Professor Dr. Kemalettin Erbatur

Keywords: Humanoid, Biped, Pushing Control, Full-Body Motion Control, Ground Interaction Forces, Balance Control, Zero Moment Point

Humanoid robots are designed for a future world where they act in a multiplicity of roles in the human environment. Imitation of human kinematic arrangement and size lends the robot ability of reaching, manipulating and operating user interfaces and tools designed for humans. The field is rich and vast covering subjects of soft robotics and safety for robot-human coexistence and cognitive research for conditional awareness and planning. This thesis deals with the force interaction of the robot through its hand end effectors. The emphasis is on applying force to an immovable object.

Pushing a tool or an object in the robot hand against a fixed surface has many application places in the industrial environment. Exertion of highest force achievable with the available mechanical system and actuators is desired. The bipedal structure, however, poses balance restrictions on the humanoid robot. When the hands push the reactive forces can cause the robot loose balance and fall.

The advantages of the bipedal humanoid robot structure in the human environment are accompanied by serious control challenges due to complex dynamics and balancing requirements.

The thesis presents a full-body reference generation and control technique in which the robot maintains balance while pushing the wall in front of it. A criterion based on the Zero Moment Point concept is employed to compute leg joint references. Added to leg joint control torques are feedforward torque components obtained from the end contact force references. These additional components are computed using optimized foot-ground interaction forces. Robot arms are controlled over hybrid position-force control. Various reference synthesis and control modes are coordinated for leaning on the wall and enlarging the support polygon on the ground.

A full-dynamics three-dimensional simulation and animation environment is employed for the development and tests of the proposed technique.

ÖZET

GÜÇ KONTROLÜ UYGULAMALARI İÇİN İNSANSI ROBOTUN KOL BACAK KOORDİNASYONU

BUĞRA SARAÇ

MEKATRONİK MÜHENDİSLİĞİ YÜKSEK LİSANS TEZİ, TEMMUZ 2024

Tez Danışmanı: Doç. Dr. Kemalettin Erbatur

Anahtar Kelimeler: İnsansı, İki Ayaklı, İtme Kontrolü, Tam Vücut Hareket Kontrolü, Yer Kuvveti Etkileşimi, Denge Kontrolü, Sıfır Momentum Noktası

İnsansı robotlar, gelecekte beşerî çevrede çeşitli roller üstlenmeleri planlanarak tasarlanmıştır. İnsanların kinematik düzenlemesini ve boyutlarını taklit etmek, robotun, insanlar için tasarlanmış kullanıcı arayüzlerine ve araçlarına erişim, manipülasyon ve işletme yeteneği kazanmasını sağlar. Bu çalışma alanı, yumuşak robotlar ve robot-insan birlikte yaşamının güvenliği ile koşullu farkındalık ve planlama için bilişsel araştırmalar gibi konuları kapsayan genişlik ve zenginliktedir. Bu tez, robotun el uç efektörleri aracılığıyla gerçekleştirdiği kuvvet etkileşimini ele almıştır. Hareketsiz bir nesneye kuvvet uygulanması hedeflenmiştir.

Robotun elindeki bir araç veya nesneyi sabit bir yüzeye itmesi, endüstriyel ortamda birçok uygulama alanına sahiptir. Bu çalışmada, mevcut mekanik sistem ve aktüatörlerle elde edilebilecek en yüksek kuvvetin uygulanması amaçlanmıştır. Ancak, iki ayaklı yapı, insansı robotun dengesini sınırlamaktadır. Ellerle itme esnasında oluşan tepki kuvvetleri, robotun dengesini kaybedip düşmesine yol açabilir.

İki bacaklı insansı robot yapısının beşerî çevredeki avantajları, karmaşık dinamikler ve denge gereksinimlerinden kaynaklanan ciddi kontrol zorluklarını beraberinde getirir.

Bu tez, robotun önündeki duvarı itme işlemi sırasında dengeyi korurken kullanılan tam vücut referans oluşturma ve kontrol tekniğini incelemiştir. Bacak eklem referansları hesaplamak için Sıfır Moment Noktası konseptine dayandırılmış bir kriter kullanılmıştır. Bacak eklemleri kontrol kuvvetlerine, son temas kuvveti referanslarından elde edilen beslemeli tork bileşenleri eklenir. Bu ek bileşenler, optimize edilmiş ayak-yer etkileşim kuvvetleri göz önünde bulundurularak hesaplanmıştır. Robot kolları, hibrit konum-kuvvet kontrolü üzerinden kontrol edilmiştir. Duvara yaslanma ve yerde destek poligonunu genişletmek amacıyla çeşitli referans sentezleme ve kontrol modları koordine edilmiştir.

Önerilen tekniklerin geliştirilmesi ve test edilmesi amacıyla, tam dinamik üç boyutlu simülasyon ve animasyon ortamı kullanılmıştır

TABLE OF CONTENTS

LIST OF TABLES

LIST OF FIGURES

1.   INTRODUCTION

Humanoid robots are made for a future in which they interact with human environment in a variety of ways. The main motivation is the idea of improving a technology that can integrate environment effectively likely a human. Biped robots are more convenient among all types of mobile robots as result of the imitation of human kinematic arrangement and size which provide capability of reaching, manipulating and operating user interfaces and tools designed for humans. The field encompasses a broad spectrum, including areas such as soft robotics, safety protocols for human-robot interaction, cognitive research concerning conditional awareness, and strategic planning. Therefore, biped humanoid robots have been developed to be used in variety of areas such as human cooperation for daily activities. Toyota Motor Cooperation has started the project "Toyota Partner Robots" to assist people in daily activities as household chores, medical care, nursing and short distance personal transportation as well as the entertainment purposed performances such as violin playing robot (Kusuda, 2008). Also, Honda projects had a great impact on humanoid robots. The motivation of those projects is to design humanoid robots that could cooperate with the human beings. This attempt led them to announce the first autonomous humanoid robot P2 (Hirai, 1999). Additionally, Boston dynamics have designed PETMAN (Nelson et al., 2012). PETMAN was designed for operating in dangerous chemical environments that are problematic due to chemical exposure issues for human. Atlas (Nelson et al., 2019) has been developed for achieving stable locomotion in complex conditions along with higher cognitive capability. These instruments have been designed to have the robot which is capable of working in military and rescue operations. HRP project (Kaneko et al., 2019) has been started to perform in industrial places which is planned to accomplish industrial tasks such as assembly and drilling with the tools designed for humans thanks to the capability and suitable design of hand end effectors, stated in Kaneko et al., 2008.

This thesis focuses on the force interactions of robots using their hand end effectors, with a particular emphasis on applying force to immovable objects. The act of exerting force against a fixed surface, using a robot hand is extensively utilized in industrial contexts. Maximizing force output within the constraints of available mechanical systems and actuators is a primary objective.

However, the humanoid robot's bipedal configuration imposes inherent challenges related to balance. The application of force through the hands can lead to reactive forces that jeopardize

the robot's equilibrium, potentially resulting in instability and subsequent loss of balance. The benefits offered by the bipedal humanoid robot structure in human environments are counterbalanced by significant control challenges arising from intricate dynamics and demanding balance requirements.

Balance requirements can be accomplished by keeping Center of Mass (COM) and Zero Moment Point (ZMP) inside the support polygon as a common practice to prevent falling down as well as stable walking reference generation (Stephens & Atkeson, 2010). Despite balance criteria as mentioned above, appropriate mathematical model is required for linearization and dealing with high dimensional state of humanoid robots due to presence of large numbers of joints. Linear Inverted Pendulum Model (LIPM) is one of the popular methods, which is used in many projects such as HRP-4 (Caron et al., 2019), that deals with simplification and the linearization of a system.

The thesis presents a comprehensive method for generating and controlling full-body references for a robot engaged in maintaining balance while exerting force against a wall. The method utilizes a criterion based on the Zero Moment Point concept to calculate leg joint references. In addition to control leg joint torques, feedforward torque components derived from desired end contact force references are incorporated. These components are computed using optimized foot-ground interaction forces. Control of the robot's arms are conducted by using a hybrid position-force control strategy. Multiple control modes and reference synthesis are coordinated to enable the robot to lean against the wall effectively and expand its support polygon on the ground.

A comprehensive three-dimensional simulation and animation environment based on full dynamics is utilized for developing and testing the proposed technique.

This thesis is organized as follows. The next chapter surveys humanoid robot projects and full-body motion control algorithms in the literature. Chapter 3 describes the humanoid robot simulation environment. The force application control design is presented in Chapter 4. Simulation results are given in Chapter 5. Chapter 6 concludes the thesis with future works.

2. SURVEY

2.1   Humanoid Robot Projects

Humanoid robots have been studied by researchers for more than 80 years in modern ways throughout the world. However, the history of humanoid robots reaches back into 15th century of Europe. Famous artist Leonarda DaVinci created the earliest version of humanoid mechanism in 1495 believed that was for a ceremony in Milan. The mechanism could stand, sit, and maneuver its arm with the operation of pulleys and cables (Capello et al., 2005). In the 18th century a series of automated dolls called "Jaquet-Droz Automata" consisting of "The Musician", "The Draughtsman", and "The Writer" are created by Jaquet-Droz family. With their winded mechanisms The Musician could play organ, The Draughtsman could draw 4 images and The Writer could even write random text 40 letters as the most complex one (Akhtaruzzaman & Shafie, 2010). Same as DaVinci's mechanism, Jaquet-Droz Automata was created for entertainment and advertising purposes. The first humanoid robot used for its functionality invented by John Brainerd called "Steam Man" in 1865. The robot was moving by its steam engine and used for pulling carts. Electrical versions of the Steam Man built by Frank Reade Jr. in 1885 called "Electric Man" (Chevallereau et al., 2009).

Figure 2.1 DaVinci's Mechanism (Left) (Wikipedia Contributors, 2019), Jaquet-Droz Automata (Middle) , The Writer's Mechanism (Right) (Wikipedia Contributors, 2019)

The groundwork for current research on humanoid robots was originated after the 20th century. In 1967, Professor Ichiro Kato launched his investigations at Wesada University with the Wesada Legged Robots (WL) family, and he conducted these research efforts until 2004. First developed one was in 1967, WL-1 (Lim & Takanishi, 2007). In 1969, WL-3 was then released. The electro-hydraulic servo-actuator of the mechanical lower limb model, the WL-3, was developed utilizing the master-slave control method. It was capable of maneuvering in both the swing and stance phases in a similar way like a human. Furthermore, it has the ability to sit and stand ("Biped Walking Robot", 2007). Rubber-based artificial muscle was first introduced in 1969 through the WAP-1. The pneumatic, anthropomorphic pedipulator, WAP-1 was developed. Rubber-made artificial muscles were connected to it as actuators. Its artificial muscles have been controlled by training and replay to achieve planar bipedal movement. The first artificial muscle of the pouch type introduced in 1970 was WAP-2 which was actuated by high power artificial muscles. By the insertion of pressure sensors beneath the soles, automatic posture control was accomplished. A more advanced version of the WAP-2 was revealed in 1970 as the WAP-3. It could walk on a level surface, climb and descend a stairway, and turn while walking since it could change its center of gravity location towards frontal plane. The latest version WAP-3 was controlled by a memory-based controller and PWM actuators are used. The first in the world was the three-dimensional automatic biped by the WAP-3. In the meantime, WL-5 was developed which was the minicomputer-controlled model. The center of its gravity was able to move on a frontal plane thanks to the laterally bending body.
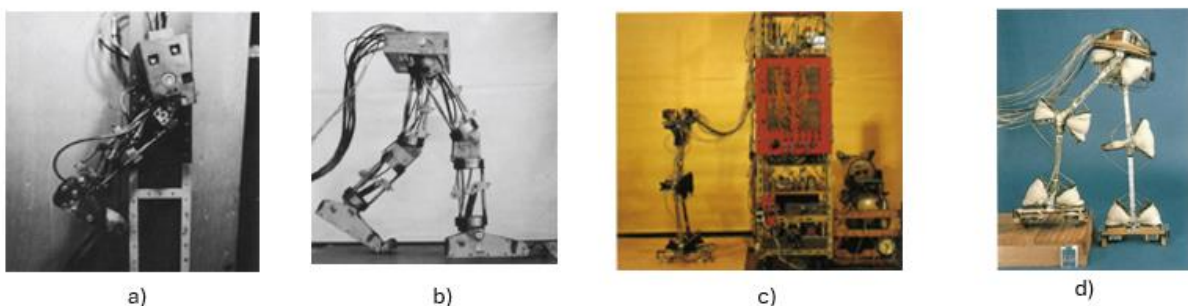

Figure 2.2 a) WL-1, b) WL-3, c) WAP-2, d) WAP-3 ("Biped Walking Robot", 2009)

WL-5 was aimed to be used to create the foundation of WABOT-1 which will used in the robot as a lower limb(45sec/step) ("WAseda ROBot", 2010). The model called WL-9DR was the first example which introduced quasi-dynamic walking in 1980. It used a microcomputer which was 16bit rather than enabling versatile control. After the conducting studies the WL-9DR's sole then touched the ground four times unlikely the previous three. Thanks to this development, the mathematical solution for a walking pattern became more accessible (10sec/step). In 1983, the WL-10R model was designed as an improved version of the previous model. It has the rotaries type servo-actuator (RSA) and structural sections made of carbon fiber reinforced plastic (CFRP). In addition to the previous model, the WL-10R added one extra degree of freedom at the yaw axis of the hip joint. Finally, the WL-10R managed to walk laterally, turning and walking forward and backward, which are called plane walking (4.4 sec/step). In 1984, the developed model of WL-10R, WL-10RD's torque sensors were connected to the ankle and hip joint to create flexible control on a change-over phase (the transition-phase from standing on one leg to switch on another) thanks to torque feedback. Eventually, all research conducted on the models succeeded in dynamic complete walking for the first time in the world with 1.3sec/step (Biped Walking Robot, 2010).
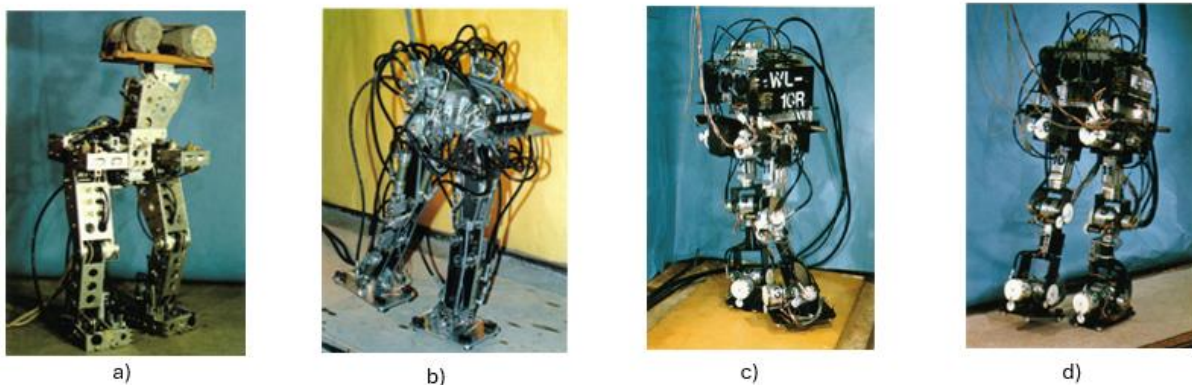
Figure 2.3 a) WL-5, b) WL-9DR, c) WL-10R, d)WL-10RD ("Biped Walking Robot", 2009)

WABIAN which is a biped humanoid robot with human configuration was developed under 5 stepped design plans to study on a cooperative dynamic walking and collaborative work with humans in 1996. 5 steps were initiated around major key points specified by Lim & Takanishi, 2000, such as the size, trunk and arm numbers, electrical issues, and approximate speed and computerized control. The model was developed in 1997 under the name of WABIAN-R to explore robot environment interaction. Afterwards, motorized joined numbers increased in WABIAN-RIII. This also presented emotional motion. Takanishi et al. indicated that WABIAN-RIII was created, in 2004, to manage the impact forces occurring between the

foot and the ground during landing. The control method allowed for the adjustment of impedance, simulating the muscle tension and relaxation in humans. The bipedal robot's movement pattern, which included a trunk, was further refined using visual and auditory sensors.
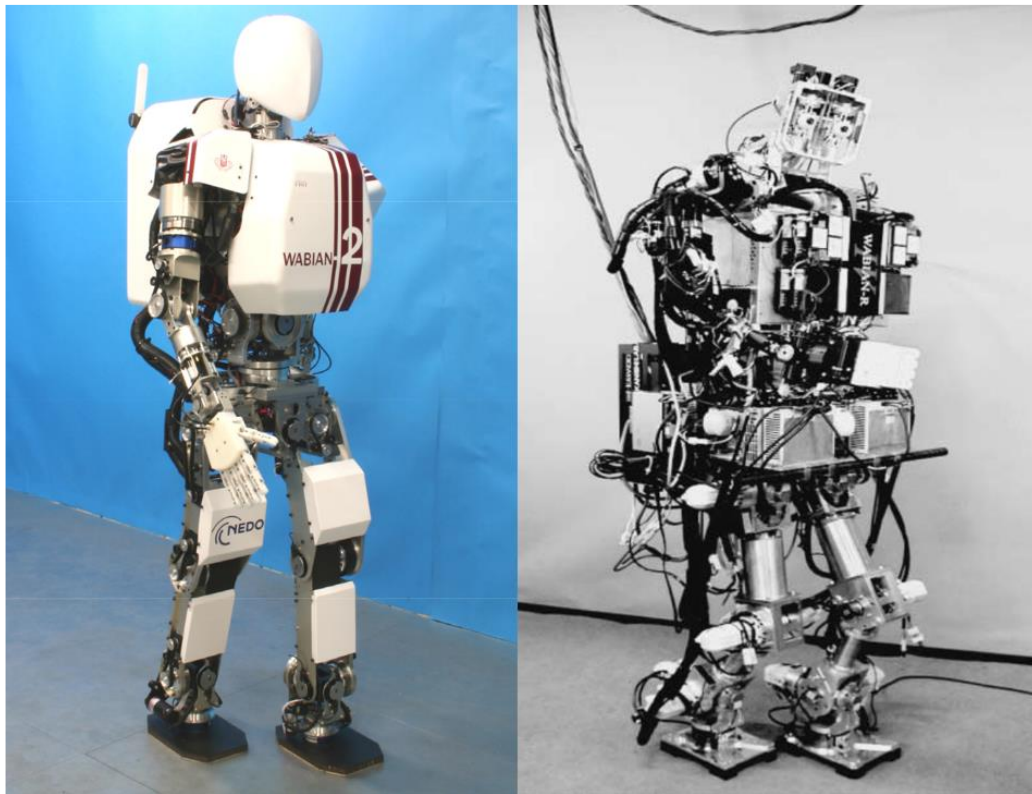
Figure 2.4 WABIAN versions WABIAN-RII on the left and WABIAN-RIV on the right(Yu Ogura et al., 2006)

Starting from 1986, HONDA have started studies on humanoid biped robots which includes 2-leg static walking robot E0 to the company's most intelligent robot ASIMO (Advanced Step in Innovative MObility). In the beginning of the company's journey, researchers have conducted with experimental models of robots with the E series along with E0 to E6. Until the model E3, the main focus was to simulate simple human walking by developing legs. Walking stabilization and more complex tasks such as climbing have been established with the continued models E4 to E6 (Narang & Singh, 2014). In 1996 first humanoid robot and the earliest version of P-series (P1-P3) of HONDA has been developed, called P1. Firstly P-series planned to be built with two-wheel mechanism which includes cameras and several sensors to develop intelligence, recognition and even decision-making as main motivation. However, it is changed with the foundation of bipedal walking comes from E0-E6 and creates P2 known as world's first autonomous humanoid robot. Even though, its reputation around the world P2 has

some problems according to its sizes. It was considered as too big and heavy for human environments with 182cm in height and 210kg in weight also it causes energy consumption problems (2750W by walking). The Robot could operate only 15 minutes even with its 20kg batteries. So that, P3 has been introduced in 1997 with smaller size (160cm in height and 130kg in weight) by conserving P2's functionality in all aspects with significantly lower energy consumption as 786W (Hirai, 1999). In 2000, the first version of ASIMO has been published as the most intelligent and suitable humanoid robot of HONDA. The robot was 120 cm tall and weighs 43kg which results in better fit in human environments as well as greater functionality with the help of i-WALK technology. The technology provides ability of walking, running while changing directions in a sophisticated way in that time (Hirai et al., 1998)
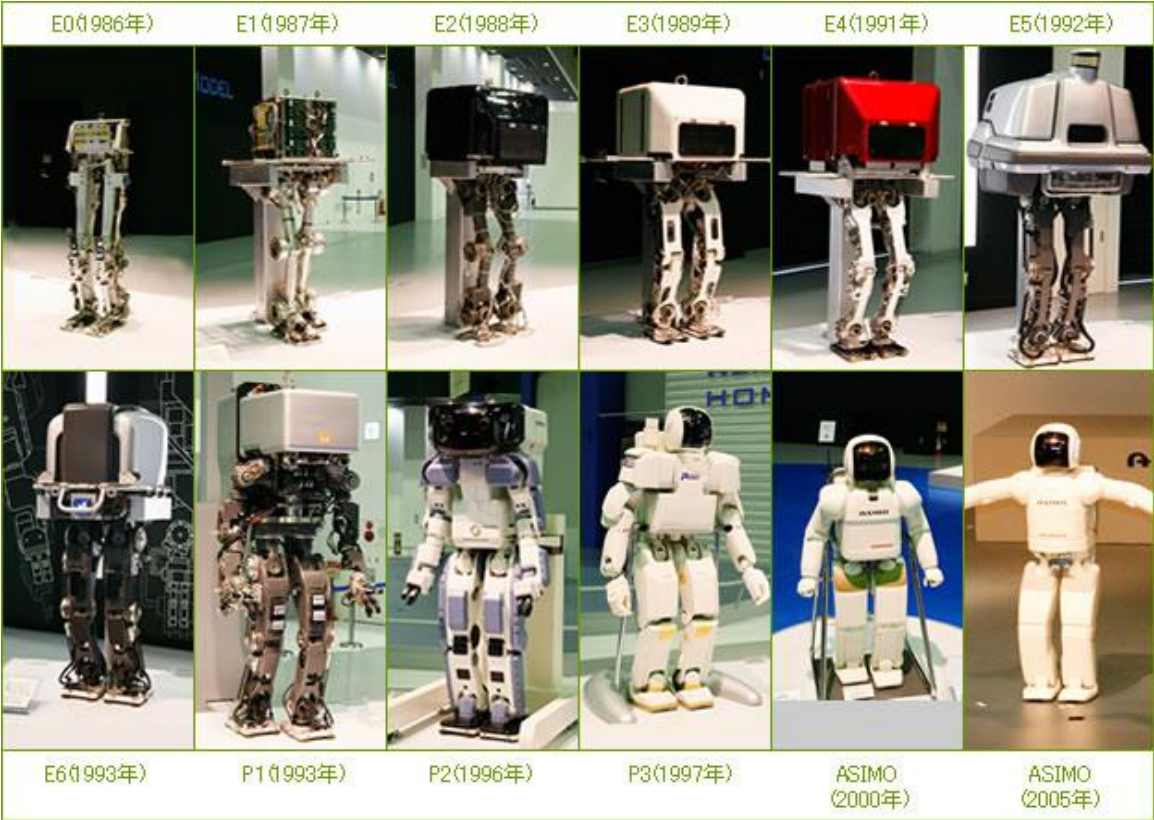
Figure 2.5 Humanoid Robot History of Honda | E0-E6 | P1-P3 | ASIMO
(ASIMOの祖先・兄弟10体が休息する空間, 2024)

The Humanoid Robot Project (HRP) was established in 1998 by the Japanese Ministry of Economy and Industry with the goal of researching and developing humanoid robots that can carry out physical tasks in the workplace (Figure 2.6). The HRP-1 prototype was developed by Honda Research and Development as an enhancement of the Honda P-3 prototype (Hirukawa, 2007). The Humanoid Research Group of the National Institute of Advanced Industrial Science and Technology (AIST) and Yaskawa Electric Corporation have collaborated

to develop the HRP-2. HRP-2 can walk in tight spaces, handle uneven terrain, walk at a pace that is two thirds of a human, lie down, and get back up on its own. Its body has been designed to resemble a human's by doing away with a backpack to house the electronics. The model HRP-3, which is created later, is heavily focused on functioning in harsh outside conditions. It has the functionality to perform in rain thanks to its waterproof mechanical and electrical structure.

Figure 2.6 HRP-2 Assembly Task with Human Assistance (Left) (Hirukawa et. al., 2004), HRP-2 Opening/Closing Valve (Middle) (Alarmy, 2024), HRP-2 Drilling Operation (Right) (GettyImage, 2007)

Although, HRP series robots are qualified to work in human environments, physical ability to work on actual sites by itself is not enough. Generally human assistance is required to complete tasks such as cottage assembly as shown in the figure (Figure 2.6). To overcome this situation, HRP-5P was developed in 2018 with electrically actuated high-power joints, redesigned arm configuration for improved physical ability (Kaneko, 2019).

Figure 2.7 HRP-5P Performing Assembly Task without Human Assistance (Kaneko, 2019).

PETMAN is a humanoid robot which has been designed by Boston Dynamics starting from 2009 to perform in chemical environments for testing chemical clothing equipments of USA Army. Individual Protective Equipment (IPE) have been tested in controlled environments in terms of wind and temperature conditions. Robot has performed basic physical task while being exposed to chemical agents. Through the chemical and variety of sensors located in the

skin (human clothing) of the robot, the location, timing and the presence of chemical agents are determined. It was asked to Boston Dynamics to deliver it in a relatively short time as 3 years. The robot should have been capable of performing in specific chemical environments with human like clothing including rough military boots as well as dynamically balanced human-like gait (Nelson et al., 2012).
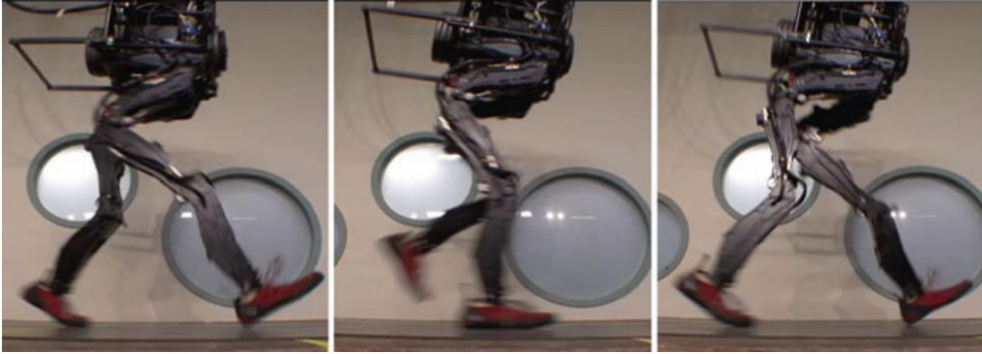
Figure 2.8 PETProto walking in a natural way on a flat surface (Nelson et. al., 2018)

Therefore, as an early stage of the project, simple biped PETMAN Prototype (PETProto) has been developed from Boston Dynamics existing BigDog (Raibert et al., 2008) hardware consisting of two, five degrees of freedom (DoF) legs. PetProto is constructed 1.5 meters in height and 44 kg in weight besides of 40kg loading capacity and its hips that has 19 centimeters lateral separation located around 1 meter from the ground surface. PetProto could perform dynamic, high speed and smooth bipedal walking gait with the maximum speed of 7.2 km/h with large US army boots which has 9.5cm width.
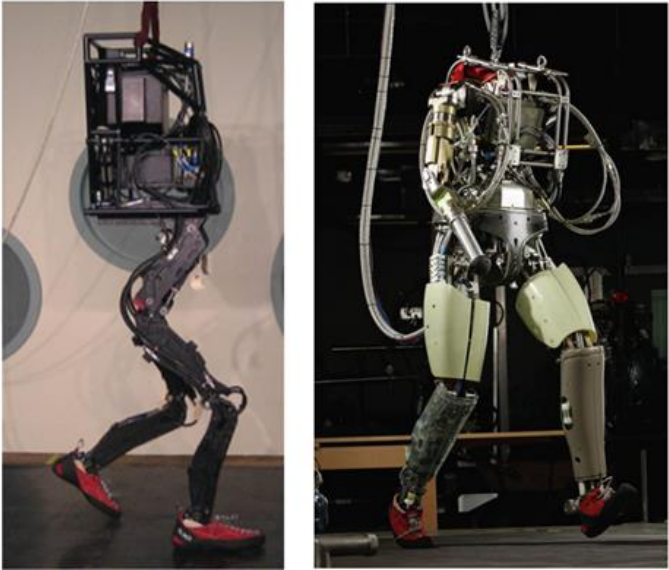
Figure 2.9 Early version, PetProto and Petman (Nelson et. al., 2018)

PETMAN has been designed in 2011 hydraulic (off-board hydraulic power unit, HPU) powered free standing biped robot. It has 140 cm height apart from the head and 80 kg weight

with additional loading capacity of 23kg. PETMAN could perform dynamically balanced heel-to-toe walking as fast as 4.8km/h. It has total 29 joints with integrated force and position sensors, are actuated by hydraulic cylinders with low-friction and hydraulic joints which are controlled by aerospace grade servo valves.

AtlasProto was constructed by augmenting PETProto with additional arms. Each arm was equipped with a shoulder joint comprising 2 DoF, an elbow joint with 1 DoF, a forearm joint incorporating a passive spring-loaded prismatic mechanism, and a simplistic "hemispherical hand." The integration of springs and sensors in the forearm joint facilitated AtlasProto's capability to detect environmental contact by its hand and quantify axial force exertion along the forearm. With AtlasProto, attention turned to two new bipedal tasks: climbing stairs dynamically and navigating a preconditioned disaster corridor obstructed by large obstacles, known as the "obstructed hallway." In both tasks, the robot employed its arms for bracing to improve balance. During climbing stairs, the robot was supported against a single wall located next to the stairs. In the obstructed-hallway scenario, the robot supported against both of the walls that framed the corridor.

Atlas has been built PETMAN's lower body with a simplified torso, articulated shoulders, and club-like arms. These arms functioned as active halteres, similar to those in insects, and played a role in controlling angular momentum. A significant improvement introduced by Atlas was the inclusion of CoP (Center of Pressure) sensing in the feet. The robot underwent several foot design iterations, three of which are listed in Table 2.1

Foot Style	Legth x Width	Weight	Tread	Sensing
PETMAN	238mm x 65mm	0.5kg	Human footwear over foam rubber faux foot	None
Atlas DRC	256mm x 121mm	2kg	"Custom replaceable Vibram® soles"	Z force & CoP via custom strain-gauge load-cells
Atlas "Duckling"	197mm x 95mm	1.4kg	"Custom replaceable Vibram® soles"	Z force & CoP via custom strain-gauge load-cells

Table 2.1 Different foot designs of PETMAN and variations of ATLAS (Nelson et. al., 2018)

The original lightweight PETMAN feet, which lacked sensors, were upgraded to larger, flat feet known as Atlas-DRC feet, featuring Center of Pressure (CoP) sensors and also used in DRC robots. This design subsequently evolved into a more compact, instrumented foot called "Duckling" for Atlas's field applications. These more robust, instrumented feet, along with the implementation of active closed-loop CoP control, significantly enhanced Atlas's standing stability compared to the PETMAN model. In the initial development phase with Atlas, two major areas of focus emerged: navigating rough and inclined terrains through reactive foot-placement control, and improving balance through better state estimation and management of angular momentum. Subsequently, a third direction was incorporated by adapting balance algorithms originally devised for PETMAN/AtlasProto to operate across multiple dimensions. This extension more explicitly integrated the concept of the "Capture Point" – a theoretical ground position where placing the Center of Pressure (CoP) of a linear inverted pendulum (LIP) would neutralize the orbital energy of the LIP with constant Center of Mass (CoM) height. The Capture Point enables the walking controller to effectively manage the dynamics of the CoM in both lateral and sagittal directions relative to ground contact forces, thereby optimizing foot placement precision for locomotive tasks such as stair negotiation, obstacle avoidance, and object   manipulation   approaches.
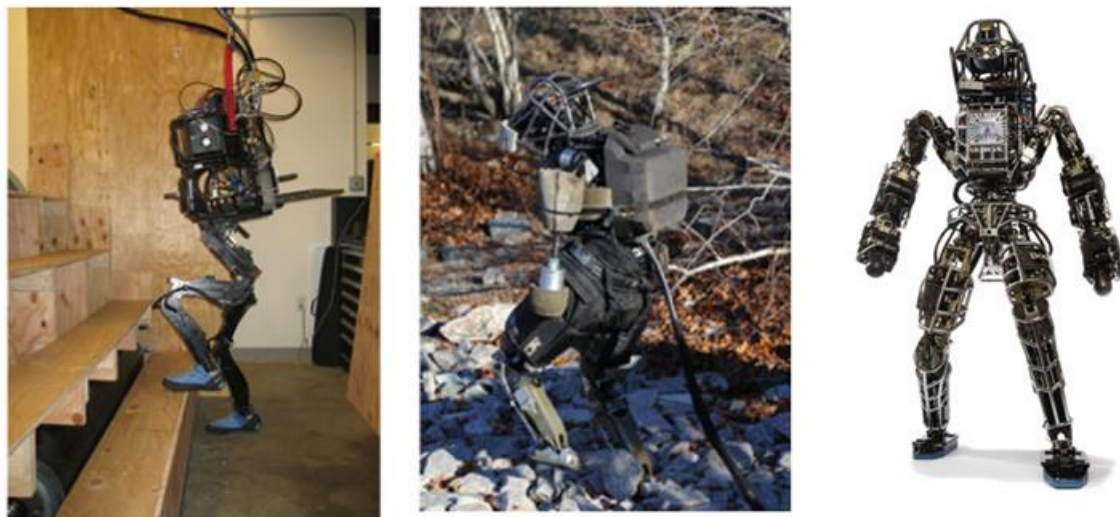
Figure 2.10 AtlasProto climbing 50 degrees of stairs (Left), Atlas walking in a rough terrain (middle), Atlas-DRC (Right) (Nelson et al., 2018)

In August 2012, development commenced on an iteration of Atlas to participate in the DARPA Robotics Challenge (DRC), an international competition aimed at advancing robotics technology. One significant hurdle for many robotics research and development teams is having access to dependable and efficient robotic hardware. To address this challenge, DARPA contracted Boston Dynamics to produce replicas of Atlas-DRC. These replicas were distributed

to selected teams in the competiton, based on their success in a robot contest executed in simulation environment. With less than a year to deliver seven robots to DRC participants, Atlas-DRC underwent a focused redesign derived from PETMAN. This redesign incorporated enhancements including more advanced arms, a sensor head, and an electrically connected Hydraulic Power Unit (HPU). The redesign process was informed significantly by ongoing rigorous testing and development of advanced behaviors on Atlas, aimed at pushing the machine's limits and showcasing lifelike motion capabilities (Nelson et al., 2018).
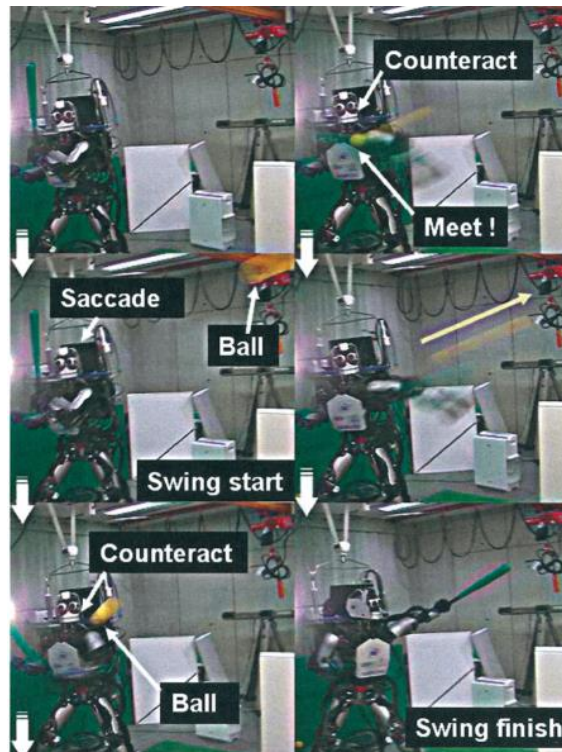
Figure 2.11 CB-i recognizes a ball thrown by a person and hitting it with a bat (Hyon et al., 2008)

CB is a bipedal humanoid robot developed by SARCOS company with following cooperators: JST (Japan Science and Technology Agency), ICORP Computational Brain Project, and ATR Computational Neuroscience Laboratories. Central pattern generator (CPG) is used in CB to perform natural humanlike walking. Joint trajectories are determined by sinusoidal with phase adjustment via coupled oscillator. Gravity Compensation-based full body force controller is developed thanks to the force controllable joints of CB (Cheng et al., 2007). SARCOS company then have been started to work on CB-i humanoid robot which can perform a baseball batting demonstration with higher cognitive capability. The robot hits a ball which is thrown by a human shown in Figure 2.11. Recognition of the wall is achieved via 4 degrees of freedom eye cameras and sequential estimator is used for arrival time estimation of the ball (Hyon et al., 2008).

2.2   Full Body Motion Control

Full body motion control is the main challenge for building a biped system because of the unstable nature of the motion. Human environment tasks require conserving the balance of the robot all the time. Biped robot has two phases for human like gait, first one is single support phase which cause an underactuated system result of less unknown variables with greater number of equations different than double support phase which causes over-actuated system result of more unknown variables with lesser number of equations (Chevallereau et al., 2013). Also, contact between foot of the biped robot and ground creates impact forces from the ground and passive DoF (Vukobratović & Borovac, 2005). High-performance balance controller is required to ensure stable human like walking for a biped robot besides the challenges of transition of phases and reaction forces from ground.

Center of Mass (CoM) and Center of Pressure (CoP) are basic concepts to describe stable and balanced dynamic system (Benjamin et al., 2010). The robot sustains its balance while keeping its CoM and CoP inside the convex hull of the foot supporting region (Feng et al., 2016). Zero Moment Point (ZMP), firstly introduced by (Vukobratovic et al., 1975), is another standard to maintain stability of a humanoid robot and controlling the position of ZMP provides balance throughout the walking. ZMP is the point where the moment generated by reaction force and reaction torque are zero. Balance of the biped robot is conducted if ZMP is located inside of the convex hull of the foot supporting area (Napoleon, Nakaura, Sampei, 2002).

Full-Body motion control is required to fulfillment of balancing criteria mentioned above. Due to the high dimensional state of humanoid robots caused by plenty number of joints, variety of mathematical representations are used to have simplified model. Inverted pendulum (IP) (Rohan et. al., 2018) is one of the methods that features with its simplicity. The trajectory of CoM is generated with a simplified model that as a humanoid robot is considered as concentrated mass and massless leg and joint angles are determined by inverse kinematics. One of the most popular models is Linear Inverted Pendulum Model (LIPM) which provides analytical solution for CoM trajectory due to its linear characteristics (Kajita et. al., 2003). Inverted Pendulum Model (IPM) is another model with constant leg length which makes CoM moves along an arch which ends up with simple dynamical equation without analytical solution caused by nonlinearity.

Although the simplicity of IPM and LIPM, they cannot provide a trajectory for double support phase. They can only generate the trajectory which is valid for only robot is standing on a single

leg, known as single support phase. In such gait planning methods, which considers only single support phase without double support phase assumed as instantaneous. Since, double support phase considered as instantaneous CoP and ZMP needs to move from the trailing foot to leading foot instantly, which may cause instability, during the transition between single support phase and double support phase.
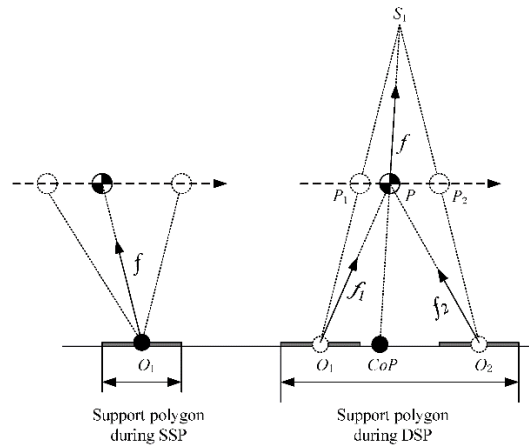
Figure 2. 12 Support Polygon and CoP during SSP and DSP (Li et. al. 2021)

The implementation of DSP is required have smoother ZMP transition caused by minimum impact between ground and foot that provides more stable and natural humanlike walking gait. In addition to that, humanoid bipedal robot has greater support polygon during double support phase (Figure 2.10). Shibuya et. al. proposed a linear pendulum model (LPM) to generate CoM trajectories in the double support phase for the horizontal ground (Shibuya et. al., 2006), which was going to be extended for more complex more complex environments (Shibuya et. al., 2008).

Improved versions of LIPM based reference generation with respect to ZMP criterion is a common practice. Since the instantaneous change of ZMP, the robot has unnatural walking gait. Erbatur et. al., proposed an application of Fourier series approximation to the dynamics equations of linear inverted pendulum model which simplifies the solution and generates smoother ZMP reference in the double support phase.

3. SIMULATION ENVIRONMENT

The following main variables can be used to describe the dynamics of a robot on legs.

$$x^T = [p_B^T, A_B^T, \theta^T] \in R^3 \times SO(3) \times R^N \tag{3.1}$$

$$v^T = [v_B^T, w_B^T, w^T] \in R^3 \times R^3 \times R^N \tag{3.2}$$

$$u^T = [f_B^T, n_B^T, \tau^T] \in R^3 \times R^3 \times R^N \tag{3.3}$$

x, v and u, represent generalized coordinates, generalized velocity and force vectors respectively. Here, p_B is a 3×1 body position vector. The body for a humanoid is typically chosen as the torso or pelvis link. The rotation matrix A_B describes the orientation relationship between the body and world coordinate frames. is a 3×3 matrix, θ is a $N \times 1$ vector consisting of joint angles, v_B and w_B are a 3×1 vectors specifying linear and angular velocities of the body respectively, joint velocities are represented in $N \times 1$ vector w , f_B and n_B are the 3×1 vectors which include forces and torques generated by body, τ is the $N \times 1$ vector consisting of joint torques generated by actuators and N is the number of joints of the robot.

The robot's equations of motion of the robot are:

$$\dot{p}_B = v_B \tag{3.4}$$

$$\dot{A}_B = A_B \times \omega_B \tag{3.5}$$

$$\dot{\theta} = \omega \tag{3.6}$$

And

$$H(x)\dot{v} + C(x,v)v + g(x) + u_E = u \tag{3.7}$$

In (3.7), $H(x)$ is the $(N+6)\times(N+6)$ inertia matrix, $C(x,v)$: $(N+6)\times(N+6)$ matrix specifying centrifugal and Coriolis effects, $g(x)$ is the $(N+6)\times 1$ gravity effect vector and u_E is the $(N+6)\times 1$ vector specifying generalized forces due to external contact forces

(3.7) is the general form of dynamic equations of the robot. A simulation environment is utilized, employing torque inputs to assess the proposed method for numerically computing joint angles and body position at each time step. The following definitions outline the procedure for simulating the biped system. At each step time, h, Euler integration iteratively updates the generalized states (x,v).

$$\boldsymbol{p}_B(t+h) = \boldsymbol{p}_B(t) + h\boldsymbol{v}_B(t) \tag{3.8}$$

$$\mathbf{A}_B(t+h) = \mathbf{T}(h\mathbf{w}_B)\mathbf{A}_B(t) \tag{3.9}$$

$$\theta(t+h) = \theta(t) + h\mathbf{w} \tag{3.10}$$

$$\mathbf{v}(t+h) = \mathbf{v}(t) + h\dot{\mathbf{v}}(t) \tag{3.11}$$

$$\dot{\boldsymbol{v}}(t) = \boldsymbol{H}(\boldsymbol{x}(t))^{-1}[\boldsymbol{u}(t) - \boldsymbol{b}(\boldsymbol{x}(t), \boldsymbol{v}(t) - \boldsymbol{u}_E(\boldsymbol{x}(t), \boldsymbol{v}(t))] \tag{3.12}$$

Where the biasing vector $\mathbf{b}(\mathbf{x}(t), \mathbf{v}(t))$ is defined as

$$\mathbf{b}(\mathbf{x}(t), \mathbf{v}(t)) = \mathbf{C}(\mathbf{x}(t), \mathbf{v}(t))\mathbf{v}(t) + \mathbf{g}(\mathbf{x}(t)) \tag{3.13}$$

Numerical integration via simulation has been described by Equations (3.8) to (3.13)

The rotating transformer $\mathbf{T}(h\mathbf{w}_B)$ in (3.9) rotates by an angle $h|\mathbf{w}_B|$ around the $\mathbf{w}_B$ axis. This transformation updates the orientation matrix of the base link based on the angular velocity of the base link.

It is derived from the equation that follows:

$$\mathbf{T}(h\mathbf{w}_B) = \left[(\cos\psi)\mathbf{I}_3 + (1-\cos\psi)\mathbf{r}\mathbf{r}^T + (\sin\psi)[\mathbf{r}\times]\right] \tag{3.14}$$

where, $\psi = h|\mathbf{w}_B|$, $\boldsymbol{I}_3$ is 3×3 identity matrix, and $\boldsymbol{r} = \boldsymbol{w}_B/|\boldsymbol{w}_B|$

The simulation calculates joint torque trajectories and ground contact forces based on the positions, velocities, and accelerations of the joint angles. Therefore, the primary objective of this framework is to generate joint torque τ and external force U_E using numerically integrated generalized coordinates x, velocities v, and accelerations $\dot{v}$.

Newton-Euler formulation (Lu et. al., 1980) can be used iteratively to determine inertia matrix $\boldsymbol{H}(\boldsymbol{x})$ and the biasing vector $\boldsymbol{b}(\boldsymbol{x}, \boldsymbol{v})$.

Biasing vector $\boldsymbol{b}(\boldsymbol{x}, \boldsymbol{v})$ can be numerically calculated by solving inverse dynamics with (x, v) set to the current state where external forces f_E and $\dot{v} = 0$. So, (3,7) can be rewritten with given $(x, v, \dot{v})$ as follows

$$u_a(x, v, \dot{v}) = H(x)\dot{v} + C(x, y) + g(x) \tag{3.15}$$

Corresponding generalized forces obtained by inertia force, centrifugal forces, Coriolis forces and gravitational forces. Computing external forces caused by environmental contact remains as a challenge to deal with. Interaction forces are obtained by an adaptive penalty-

based technique proposed by (Erbatur & Kawamura, 2003) which works with the idea of reducing kinetic energy bodies in contact. Then it is possible to obtain generalized external force u_E since external force vector f_E has been generated.

$$u_E = \sum_{j \in M_A} K_j F_{E_j} = K f_E \tag{3.16}$$

where

$$M_A = \bigcup_{i=1}^{N} M_i \tag{3.17}$$

K_j : $(N+6) \times 3$ matrix specifying transforms from j^{th} external force to generalized forces

M_A : Index numbers for contact points

f_E : Vector active contact forces vector, $(3M) \times 1$

K : $N+6 \times (3M)$ matrix which relates external forces vector f_E with u_E

M : Number of time-variant active contact points

Equations (3.7) and (3.16) can be rewritten as

$$u_A = u + K f_E \tag{3.18}$$

K can be computed through inverse dynamics with Newton Euler computations, too.

In the simulation environment used in this thesis the matrices H, b and K are all computed cyclically and used to compute robot posture and joint coordinates under actuation torques τ.

The scene of the robot is animated using OpenGL in Visual Basic. A screenshot of the animation window is shown in Figure 3.1.
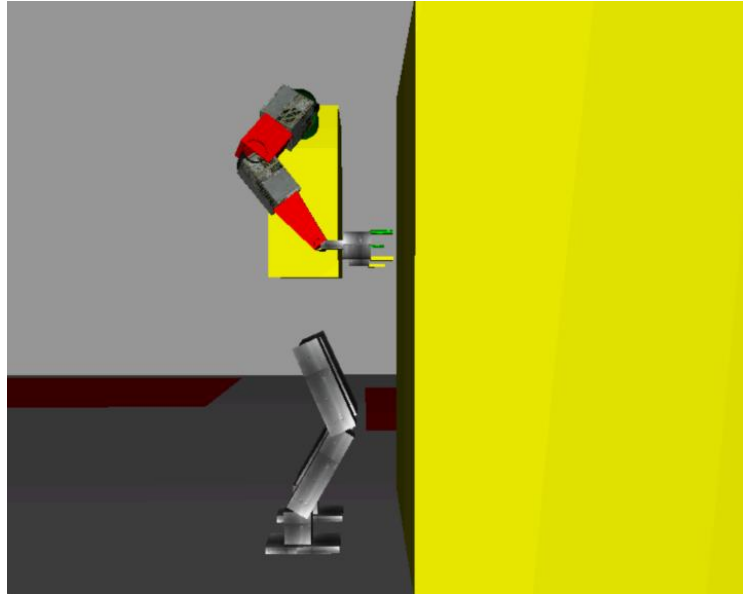
Figure 3.1 A screenshot from the animation software

Parameter values of the Sabancı University humanoid robot SURALP (Figure 3.2) are employed in the simulations.
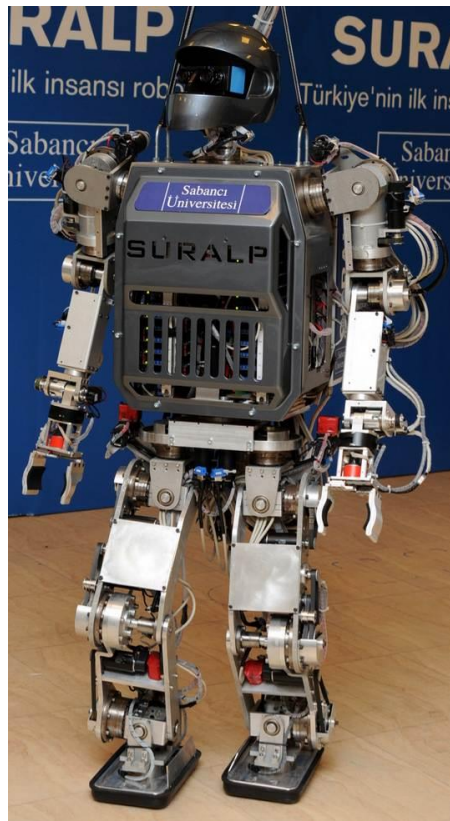
Figure 3. 2 The humanoid robot SURALP

Data of SURALP are given in Table 3.1. The robot has 29 DOF. However, 24 DoF used in this model which includes 6 DoF for each legs and 6 DoF for each arms. Joints located in hands, neck and waist are neglected in the simulation environment.

Weight	114 kg
Length of lower leg	270mm
Length of upper leg	280mm
Dimensions of foot	240mm x 150mm
Length of lower arm	255mm
Length of upper arm	219mm
Distance between Ankle center and foot sole	124mm

Table 3.1 SURALP size and weight.

4.   CONTROLLER DESIGN

In this chapter building blocks of the reference generation and control techniques employed in the thesis are described. The first two sections are related to leg walking and stance reference generation. The third section is about the reactive force scheme which provides a feedforward support to the robot body when hands are in contact with the wall. The hybrid control scheme of the arms is briefed in the fourth section. Finally, the chapter is concluded by introducing two alternative employed block diagrams which employ the techniques explained. One scheme is position based and is used when not contacting the wall. The second one uses the reactive method for legs and hybrid arm control, and is applied when arms are touching the wall.

4.1   Zero Moment Point Criterion Based Walking Reference Generation

The Zero Moment Point criterion is based on the fact that when a legged robot falls due to loss of balance, there will be a rotation of its body pivoted about one side of its foot sole. That the robot rotates about the foot sole edge is an indication that torque balance about this point is violated. If, however, torque is balanced about the foot edge, the robot is in a condition between falling and regaining its balance. Further, if the torque balance is computed about a point which is inside the sole, the robot is stable and not falling. Hence, the location this point, called the Zero Moment Point, can serve as a stability criterion for legged robots. It is successfully implemented as means of reference generation and control

Figure 4.1 shows typical setting for bipedal walk reference generation. Reference foot locations are determined first. They define support polygon location and shapes. The Zero Moment Point is to lie in the support polygon all the time for a stable walk. Therefore, a trajectory which lies in the time-varying support polygon areas is suitable for the Zero Moment Point. Having determined this trajectory is the first stage of reference generation. Next, the Linear Inverted Pendulum Model is employed to simplify the relation between the robot center of mass (CoM) and various techniques can be applied then to compute the location of the CoM. In this thesis the technique in (Kurt and Erbatur 2009) is applied for this purpose. It is based on Fourier series approximation of eriodic signals. Once the CoM location is found, the inverse kinematic between the CoM and the feet can be solved and this process yields joint angle

references. These references are followed by independent joint PID controllers to achieve walking

When the robot is stationary, that is it is not walking, still the reference generation and PID control algorithms are active to control the stance of the robot.

It should be noted that, in this thesis, there are two application places of the ZMP based reference generation and PID independent joint controllers: Standing and making one step backwards to enlarge the support polygon. These implementations are explained in more detail in the next Chapter
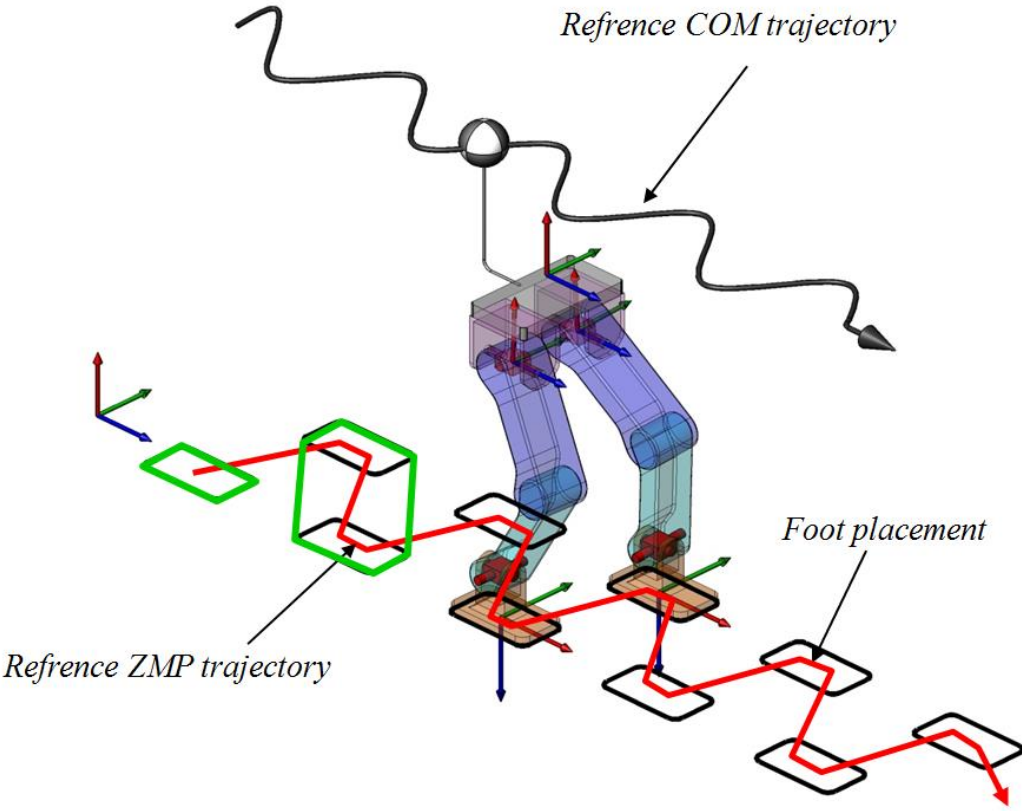

Figure 4.1 Reference generation with Zero Moment Point Criterion

4.2   Changing the Walk Plane

Changing the reference walk plane and still keeping the body posture upright is implemented in (Seven et al. 2012) for robot walk on uneven surfaces (Figure 4.2).
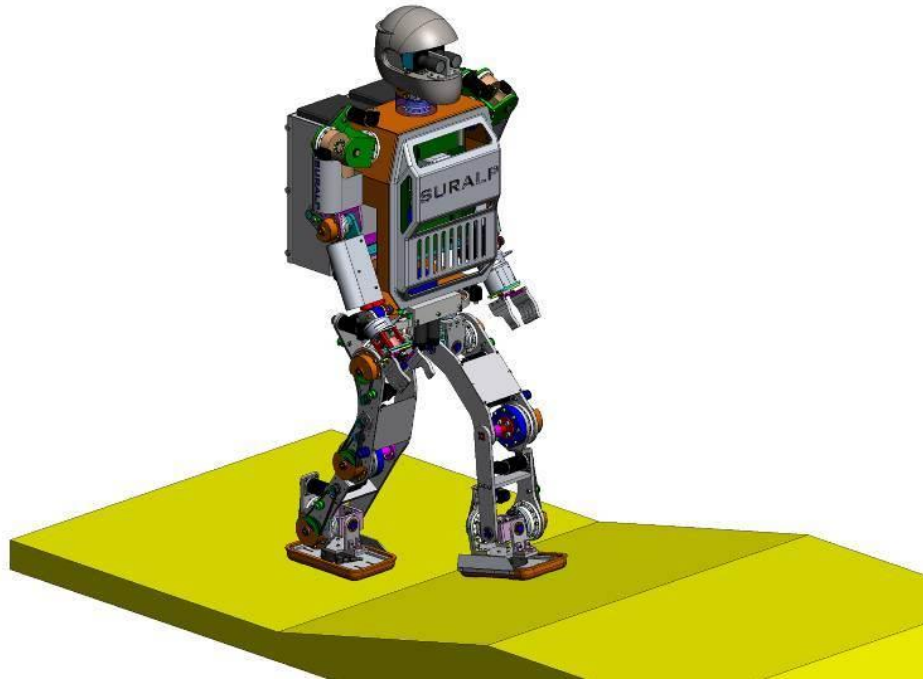
Figure 4.2 Humanoid walk on a unfixed slopped surface

The walking gait is defined according to the fixed frame called world coordinate frame is utilized to define the motion of the robot such that x-direction can refer robot's walking direction. Also, shows the coordinate frames attached to the hips and sole of the foot for foot position and orientation. In addition, a coordinate frame is located at the center of the upper body, mainly called body coordinate frame. The frames mentioned above are shown in the Figure 4.3. Although, body reference frames and the world coordinate frame are aligned parallel to each other in the beginning of the motion, several factors consisting of gravitational forces, foot ground interaction, coupling effects between the links and changing slopes affects this alignment during the walk of the robot.

Figure 4.3 Coordinate frames related with reference generation while walking. o_w is the origin of world coordinate frame and o_b is the origin of body coordinate frame.

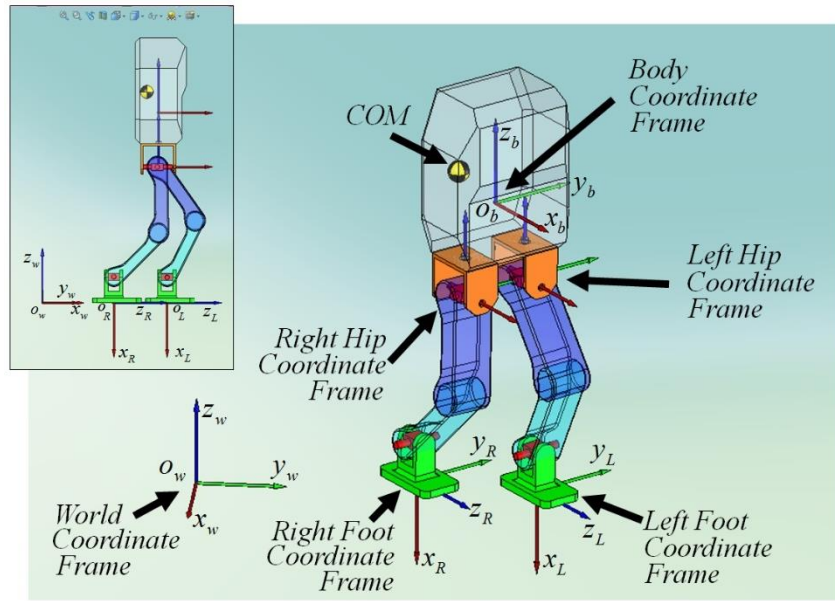Still utilizing the ZMP (Zero Moment Point) and LIPM (Linear Inverted Pendulum Model) based reference generation method for even-floor walking, as described in Erbatur and Kurt (2009) and Taşkıran et al. (2010), modifying the walking plane by rotating foot references around a pitch axis located at ground level can achieve walking on inclined planes (Seven et al. 2012). The references of foot are transformed rotationally which entails more than just adjusting foot orientations; it also alters the direction of foot motion. Following this transformation, the originally parallel motion of the foot relative to a level floor becomes aligned with an inclined plane instead (Figure 4.4)

The same computational background, however, can be exploited to maintain the feet level with the ground and cause the inclination of the body. This technique is employed in this thesis to create body inclination on flat ground and towards the wall on which force is to be exerted (Figure 4.5). Leaning on the wall makes the humanoid balance less affected form the hand-wall contact forces
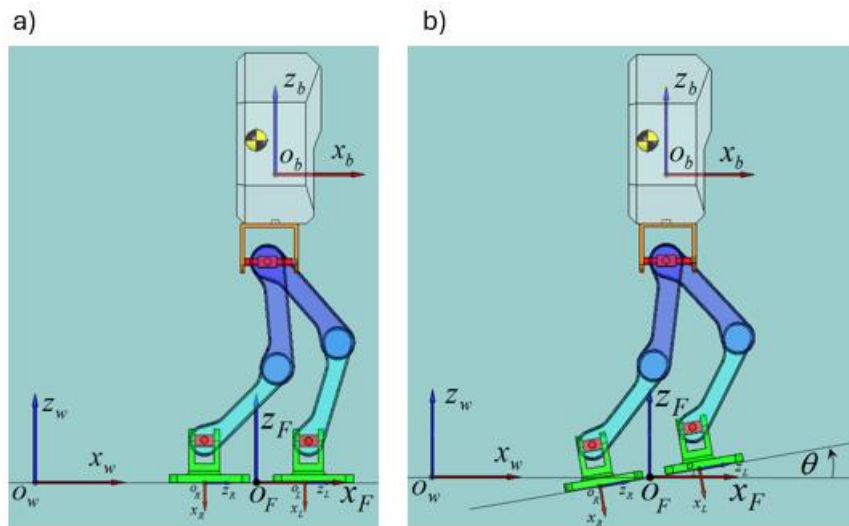
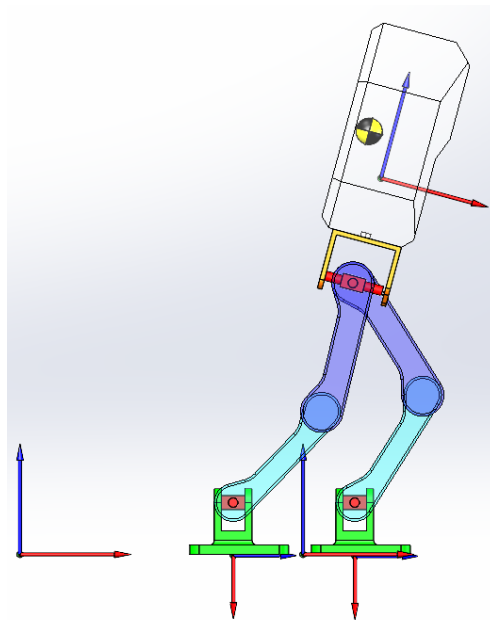Figure 4.4 Walk plane change in (Seven et al. 2012)

Figure 4.5 Inclined body on an even surface

4.3   Reactive Control

The reactive control method for legged robots is based on computing necessary contact interaction forces to create force and torque effects on the robot body. Reactive control can be used as the sole body position and orientation technique ((Ayhan 2004, Aktaş 2021)) in a control system. In this thesis, however, it is applied as a feedforward control term supporting robot balance. The body is, in effect, pushed towards the wall by a force equal to the contact force between the hands and the wall.

By decomposing the inertia matrix into sub-matrices, dynamic equations in (3.7) can be written as

$$
\begin{bmatrix} H_{11} & H_{12} & H_{13} \\ H_{21} & H_{22} & H_{23} \\ H_{31} & H_{32} & H_{33} \end{bmatrix} \begin{pmatrix} \dot{v}_B \\ \dot{\omega}_B \\ \ddot{\theta} \end{pmatrix} + \begin{pmatrix} b_1 \\ b_2 \\ b_3 \end{pmatrix} + \begin{pmatrix} u_{E_1} \\ u_{E_2} \\ u_{E_3} \end{pmatrix} = \begin{pmatrix} 0 \\ 0 \\ \tau \end{pmatrix}
\tag{4.1}
$$

The external effect generalized forces can be computed as

$$
\begin{pmatrix} u_{E_1} \\ u_{E_2} \\ u_{E_3} \end{pmatrix} = K f_E
\tag{4.2}
$$

where K is one of the matrices computed every simulation cycle via techniques references in Chapter 3. The translational and rotational dynamics for the body link can be extracted from the equation above as

$$
\begin{bmatrix} H_{11} & H_{12} \\ H_{21} & H_{22} \end{bmatrix} \begin{pmatrix} \dot{v}_B \\ \dot{\omega}_B \end{pmatrix} + \begin{bmatrix} H_{13} \\ H_{23} \end{bmatrix} \ddot{\theta} + \begin{pmatrix} b_1 \\ b_2 \end{pmatrix} + \begin{pmatrix} u_{E_1} \\ u_{E_2} \end{pmatrix} = \begin{pmatrix} 0 \\ 0 \end{pmatrix}.
\tag{4.3}
$$

The relation between contact forces and the reactive force on the body is given by

$$
\begin{pmatrix} u_{E_1} \\ u_{E_2} \end{pmatrix} = K' f_E
\tag{4.4}
$$

where K' is a sub-matrix of K. The same relation is valid for reference values:

$$\begin{pmatrix} u_{E_{1ref}} \\ u_{E_{2ref}} \end{pmatrix} = K' f_{E_{ref}} \ . \tag{4.5}$$

When the generalized forces are used as feedforward pushing supports $u_{E_{2ref}}$ is zero (torque effect on the body) and $u_{E_{1ref}}$ (force effect on the body) will be equal to the reference force value in the hand-wall contact.

(4.5) can be solved to obtain $f_{E_{ref}}$. The equation does not describe a unique solution and the solutions of the equation are not physically applicable for all times. Non-attractive nature of the contact and no-slip conditions have to be satisfied.

With $f_{E_i} = \begin{bmatrix} f_{Eix} & f_{Eiy} & f_{Eiz} \end{bmatrix}, \quad i \in \{1,2,\ldots,8\}$ (four-foot corner contact points are assumed), the constraints are

$$f_{E_{iz}} \geq 0, \quad \forall\, i \in \{1,2,...,8\} \tag{4.6}$$

$$-\mu \leq \frac{\sqrt{f_{E_{ix}}{}^2 + f_{E_{iy}}{}^2}}{f_{E_{iz}}} \leq \mu, \quad \forall\, i \in \{1,2,...,8\} \tag{4.7}$$

(4.6) is for non-attractive nature of the contacts and the constraint for no-slip is formulated in (4.7). These can be approximated (Ayhan 2004) by

$$\begin{aligned} -\frac{\sqrt{2}}{2}\mu &\leq \frac{f_{E_{ix}}}{f_{E_{iz}}} \leq \frac{\sqrt{2}}{2}\mu \\ -\frac{\sqrt{2}}{2}\mu &\leq \frac{f_{E_{iy}}}{f_{E_{iz}}} \leq \frac{\sqrt{2}}{2}\mu, \quad \forall\, i \in \{1,2,...,8\} \end{aligned} \tag{4.8}$$

(4.8) is more conservative than (4.7), however it is a set of linear constraints, and this simplifies the problem. (4.6) and (4.6) can be put into form

$$A f_E \leq 0 \tag{4.9}$$

where A is a matrix obtained from these constraint inequalities and the problem becomes obtaining $f_{E_{ref}}$ which minimizes

$$\frac{1}{2}\left\| K'f_{E_{ref}} - \begin{pmatrix} u_{E_{1ref}} \\ u_{E_{2ref}} \end{pmatrix} \right\|^2 \tag{4.10}$$

subject to $Af_{E_{ref}} \leq 0$.

This linear constrained least squares fitting problem is solved by sequential quadratic programming (Rardin, 2000). This is implemented in MATLAB and used in this thesis. The result of optimization is transformed to joint torques by:

$$u_{E_{3ref}} = K''f_{E_{ref}} \tag{4.11}$$

where K'' the sub-matrix relating contact forces to reaction forces on joints.

With

$$H_{33}\ddot{\theta} + \begin{bmatrix} H_{31} & H_{32} \end{bmatrix} \begin{pmatrix} \dot{v}_B \\ \dot{\omega}_B \end{pmatrix} + b_3 + u_{E_3} = \tau \tag{4.12}$$

the relation

$$\tau_{ref} = u_{E_{3ref}} + \hat{b}_3 \tag{4.13}$$

is used as the feedforward control torque. This torque is used in addition to the PID joint control torques obtained to track ZMP -based reference trajectories.

4.4   Hybrid Force-Position Control for Arms

When the hands are in contact with the wall, a hybrid force-position controller is invoked. The controller act independently for the two arms. The contact is modeled by one contact point per hand. A spring and damper based wall contact is modeled in dynamics simulation. When the contact point of a hand touches the wall the first instant contact position is captured. This position defines a position reference for the rest of the contact. Position control tries to keep the hand in this position in directions tangential to the wall, whereas the desired contact force is to be applied perpendicular to the wall. A proportional derivative (PD) Cartesian position controller is devised in the tangential directions. The output of this controller, together with the desired contact force in the perpendicular direction make the desired Cartesian force

on the hand contact point. This vector is multiplied by a sub-matrix of the overall environmental interaction matrix to compute the arm joint torques:

$$u_{E3ref\ arm} = K'''f_{E_{ref}\ arm} \tag{4.14}$$

4.5   Coordination of Reference Generation and Control Methods

In this thesis it is aimed to build a controller which provides the maximum force exertion capacity to the bipedal humanoid robot model. Therefore, two different controller has been designed to perform individual requirements of different simulation phases as well as the force exertion with remaining balance. These control structures are used in terms of the phases of the simulation will be discussed in the next section.

The first controller (shown in Figure 4.6) has been developed to perform stance position of the robot and to provide motion of the arms until their connection to the wall. When the robot reaches to the wall then the control structure has switched to the second one which is shown in Figure 4.7. Since there is not any force exertion before arms are contacted to the wall, both arms and legs are controlled via position control technique. However, position references of arms and legs are obtained in a different way.

Position reference of arms is given as cartesian references. The reference point determined from the location of the wall which is fixed throughout the simulation. Inverse kinematics is applied to compute required arm joint angles. Obtained joint angle references are used in independent joint PID position controller to compute torques of joints created by the motion of the arms.

Zero moment point based position reference is employed to the legs to obtain required body posture during stance position. Inverse kinematics is applied to obtain required joint angles after position references. Independent joint PID controller computed the generalized joint torques of the legs to sustain balance.

Second controller's block diagram is consisting of more complex control structure to accomplish maximum force exertion of the robot to the wall. This controller is constructed to maintain robot's balance under the effect of environmental reaction forces due to force application to the wall.

For maximizing capability of the robot in terms of applied force without falling, variety of motions and methods are employed. These are, leaning against the wall, one step backwards

28

and most importantly pelvis boost application. Flow of the simulation is shown in the Figure 5.1 described in detailed in the next chapter.

In the second control structure, hybrid position-force controller has been built for arms as distinct from the first block diagram. In this controller, position references of the arm in y and z axis are given as a cartesian position reference with respect to the pelvis coordinate frame. After errors are determined via position references in these axes, correction forces are computed by the product sum of proportional and derivative terms of the errors respectively. By this operation corrective force vector has been evaluated without x axis component. Then the reference in x axis given directly as a force reference. Eventually, corrective force vector comes up with the joint torques of the arm after $K_{t_{arms}}$ product.

Legs are controlled by position control with respect to zero moment point base position references for body posture and walking generation. In addition to that, additional force is generated by pelvis, pelvis boost, to increase force exertion capacity of the robot. This additional force capacity comes with additional required torque in legs.

Force references of the arm is multiplied by body force selection matrix S_{body}. It is a matrix that relates arm force reference with respect to x axis of pelvis frame eventually. Since, the goal is to create additional force by pelvis in x direction, which is the pushing direction of the robot, the multiplication of matrix S_{body} and force reference of arms creates a vector such consists three-dimensional force and torque reference components of the pelvis to follow force reference coming from the arms. Then, an optimization technique mentioned in Chapter 4.3 is used to determine joint toques that are applied as additional torque to the PID joint control torques obtained from ZMP - based reference trajectories.
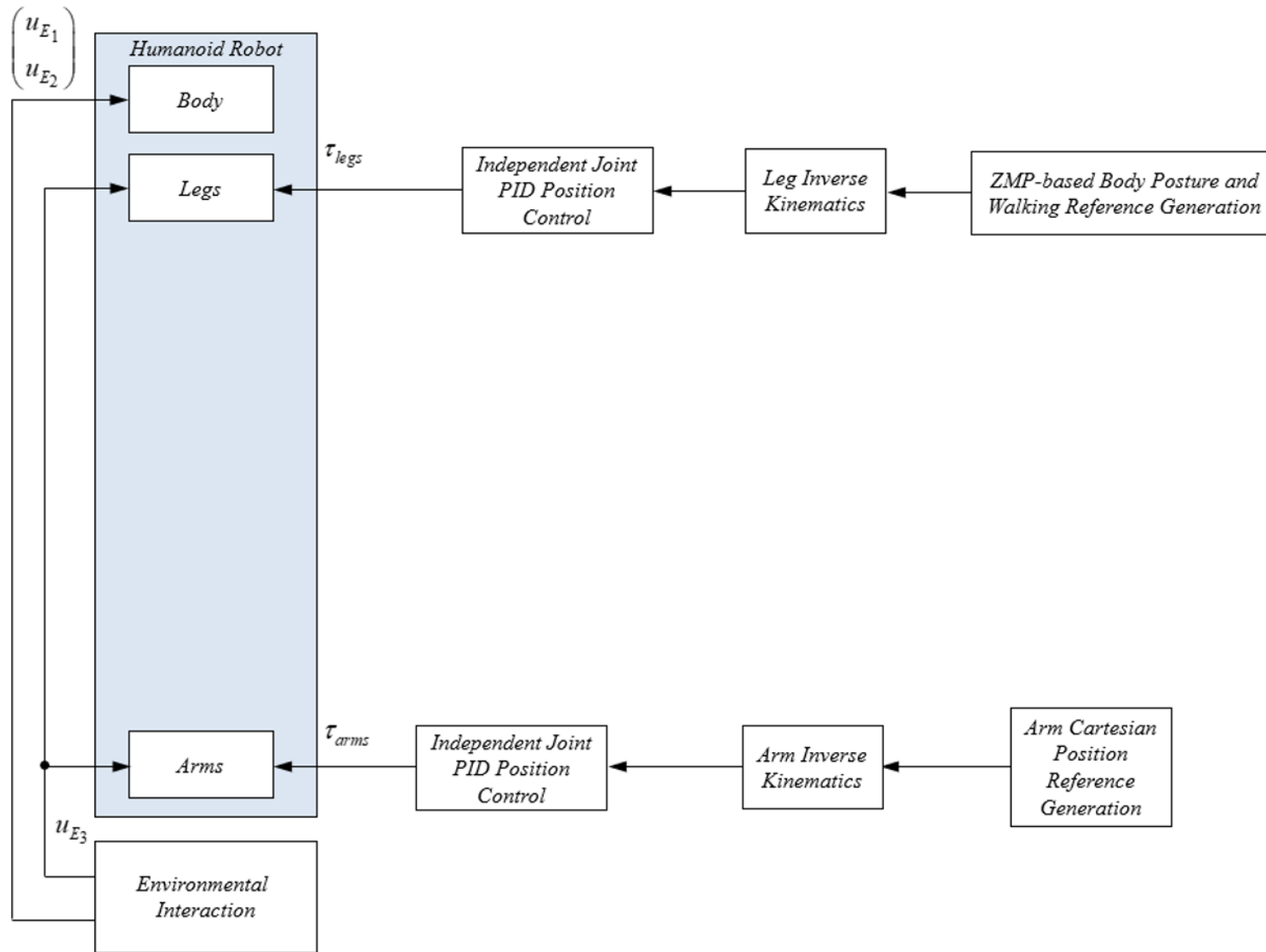
Figure 4. 6 Controller for non-contact states of the model. This controller is used only in first two phases of the simulation when the robot does not apply any force to the wall

30
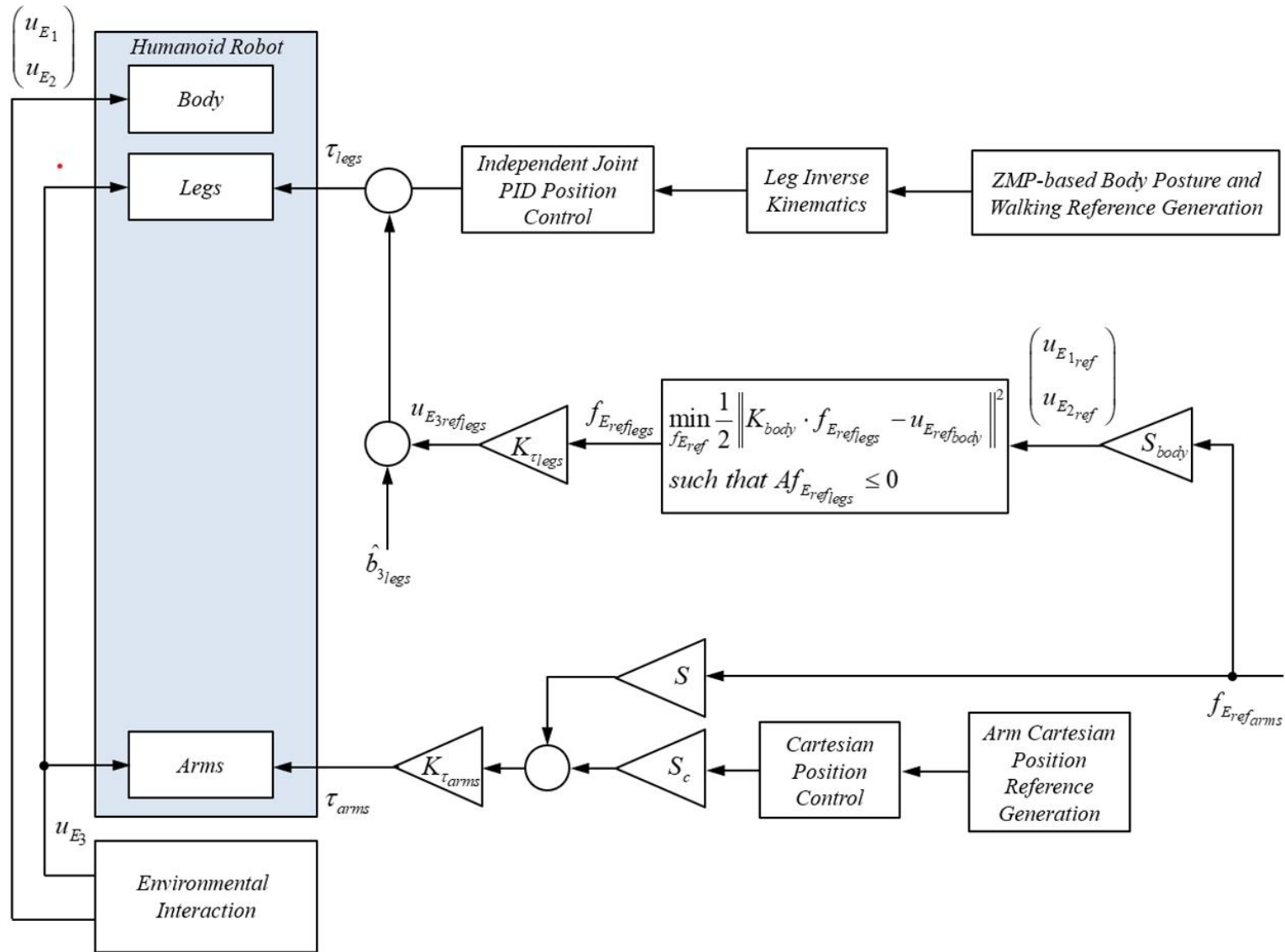
Figure 4.7 Controller for contact stated of the model. The controller is used from the beginning of phase 3, which is the first force exertion, to end of the simulation

5.   SIMULATION RESULTS

Figure 5.1 Phase diagram of the simulation

This thesis focuses on control procedure which has the motivation of exerting maximum, force to the wall by humanoid bipedal robot created in simulation environment. In order to do this, multiphase control algorithm has been created consisting of different control modes in different time intervals as mentioned in previous chapter.
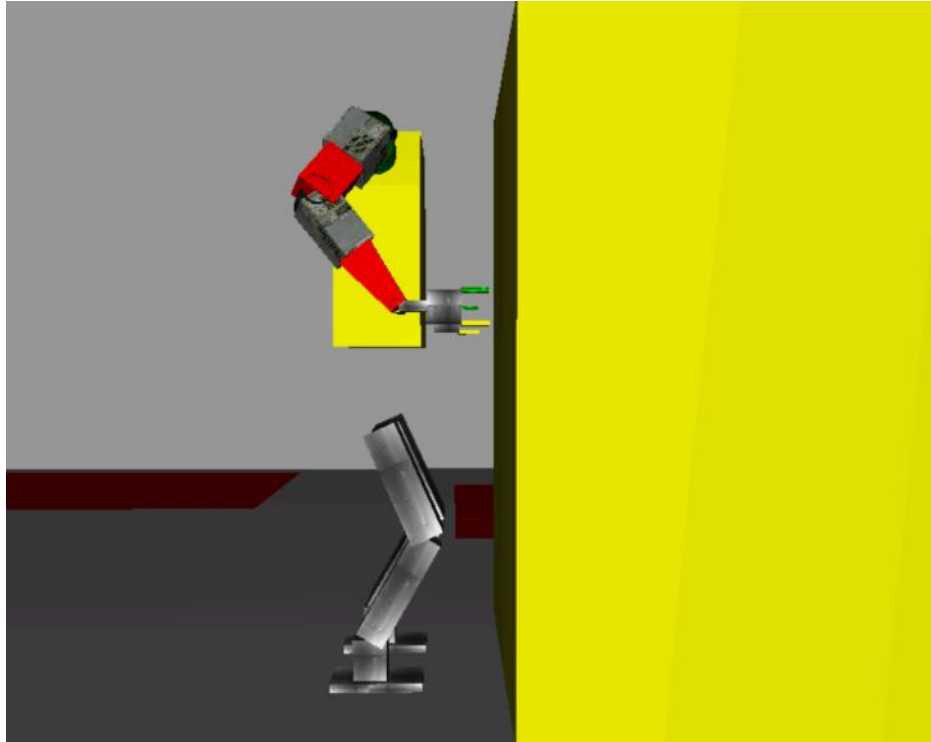
Figure 5.2 Stance position of the robot during phase 1 for 1 second
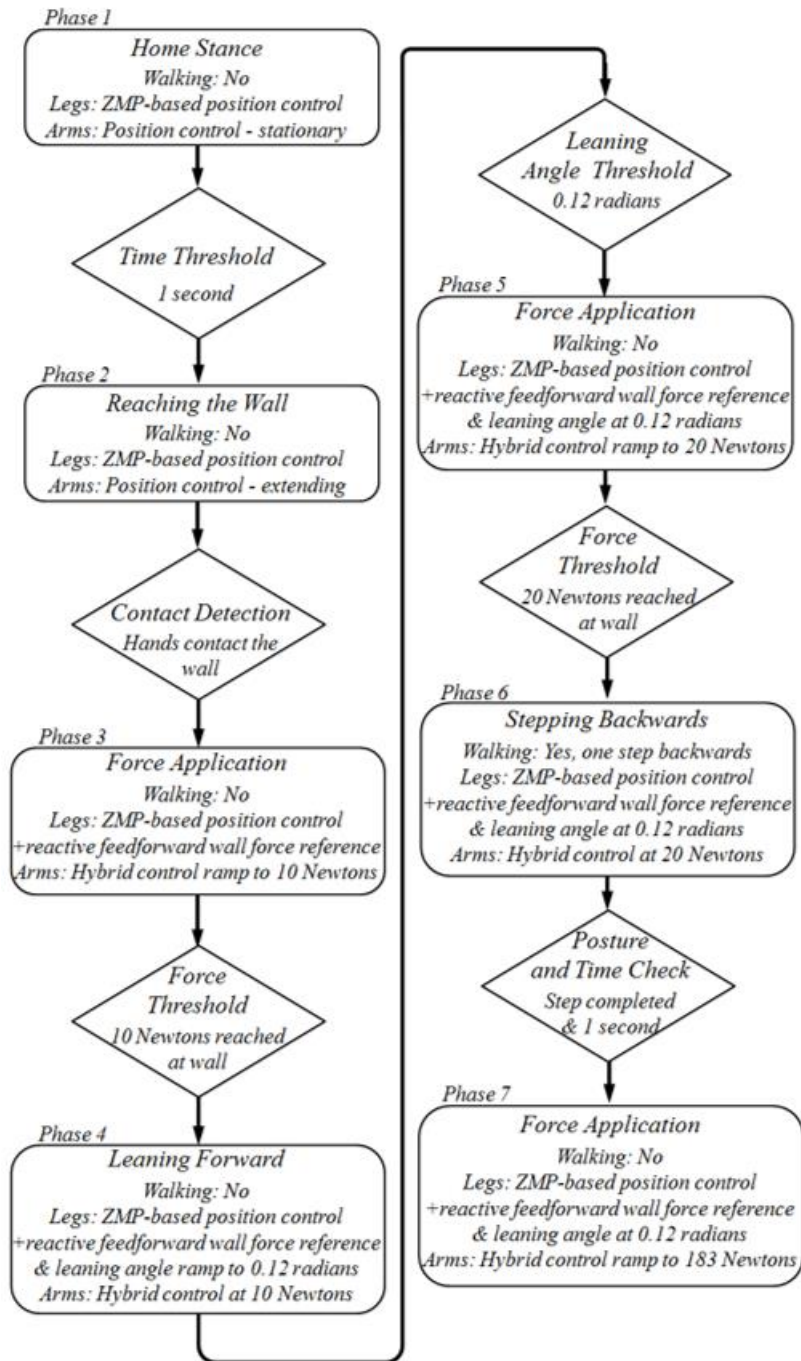
In the beginning of the simulation the robot is in the stance position for determined time threshold, 1 second. Stance position of the robot has shown in Figure 5.2. Legs are under the position control with respect to position references determined by zero moment point to sustain robot's balance. Arms are position controlled and stationary. Inherently, reaction force acted on arms are not observed during this phase as shown in Figure 5.3.

Figure 5 3 Hand contact force for both arms from phase 1 to phase 7

Figure 5.4 Robot arms achieved the first contact to the wall in phase 2

After the waiting time threshold is passed, second phase is performed to reach the wall by hand. Reaching process of the robot has been performed only by arms legs stays stationary. Contact state of the model has be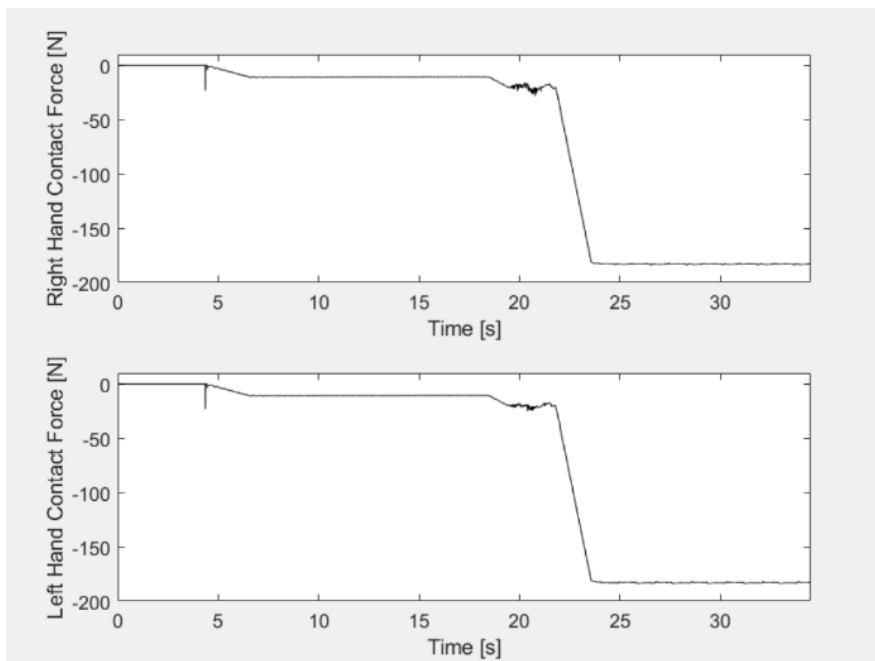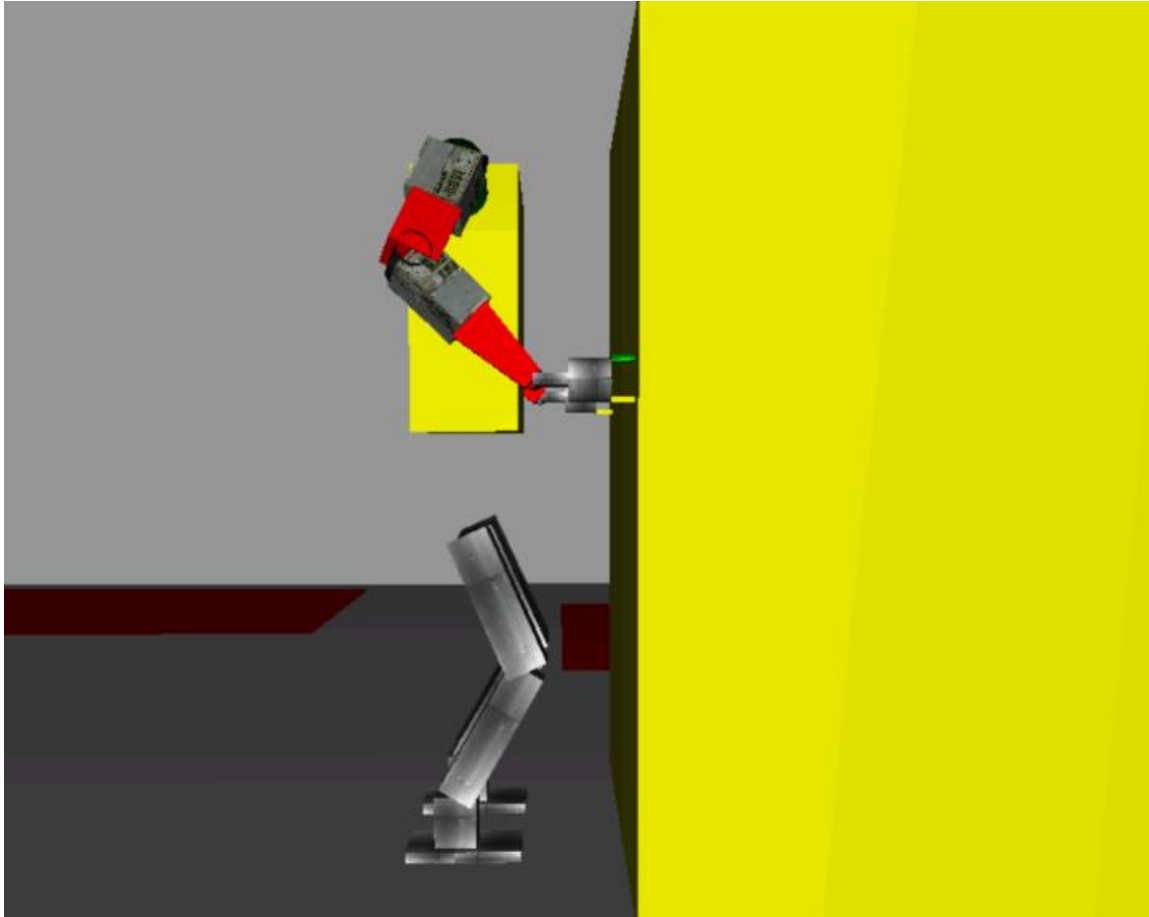en visualized via Figure 5.4. Zero Moment Point based position control applied for legs to remain steady posture. Reaching the walls performed via position control of arms with respect to the cartesian position reference which is given as a position of the wall relative to the pelvis coordinate frame. Contact of the hand to the wall is detected by the position of the hand reaches the wall position. Also, instant contact force has been detected at the point when arms contacted to the wall even there is not any force reference given. Force contact peak caused by first contact of the arm can be observed from the Figure 5.3.

Force application has been started at this point after hand of the robot contacted with the wall in the second phase. In this phase arms controlled by a hybrid controller due to required force exertion. The hybrid controller of the arm works with position references of the hand in z and y axis. Reference in x axis given as a force reference, 10 Newtons, with ramp. Consequence of ramp applied as reference force can be observed from hand contact forces shown in Figure 5.3. Hand contact force increased from 0 Newtons to 10 Newtons smoothly. The practical function

of the force applied on the wall in this phase is to prepare robot for next phase which is leaning against the wall. So, reactive feedforward wall reference acted on legs to create additional force from the pelvis, is not actually affect the performance of the robot in this phase.

Figure 5.5 Leaning to the wall is performed in phase 4

After the force reference, 10 Newtons, is applied to the wall, the fourth phase has started. The amount of force applied in previous phase is determined experimentally. Leaning forward without applied force towards the wall, robot has lost its balance and eventually fallen. In this phase, its planned to make the robot lean against the wall (Figure 5.5) to shift its center of mass closer to the wall. Thus, the robot becomes more resistant to the reaction forces of the wall caused by the force applied on it. Throughout this process, wrist joints rotated by 0.12 radians with a ramp. Applied force to the wall is not increased, remains same within phase three. Legs of the robot are controlled with position control same as before.
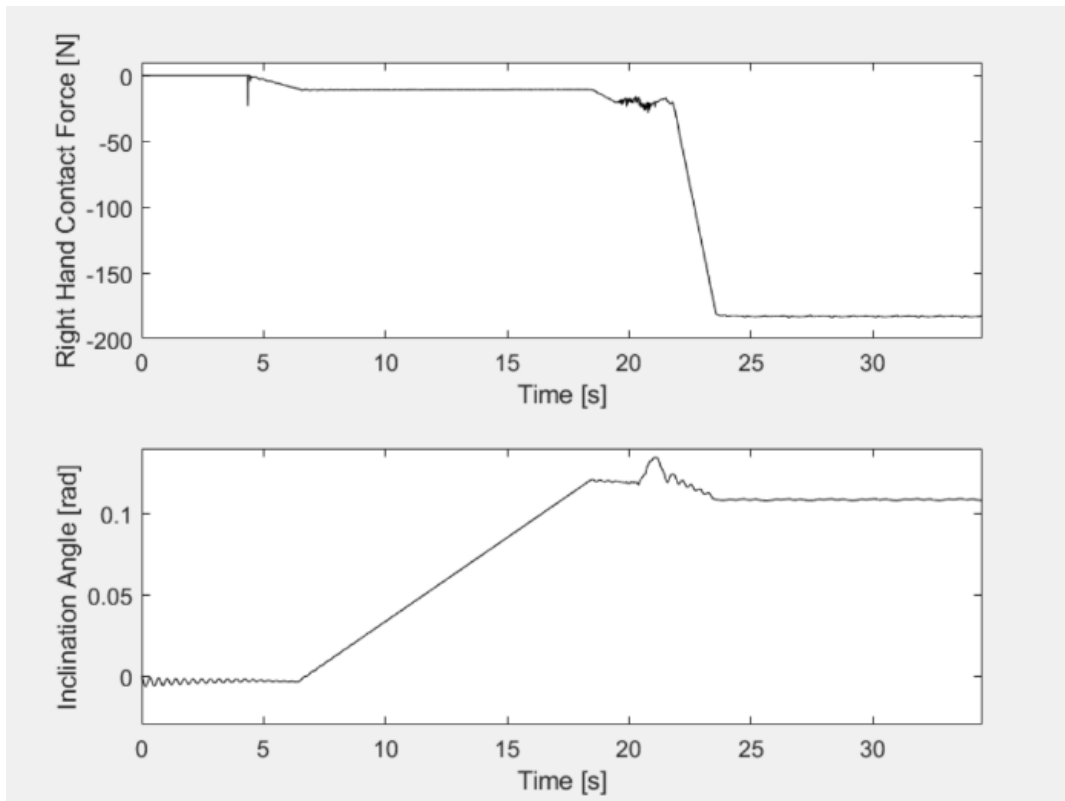
Figure 5.6 Plot of the inclination angle with hard contact forces

Figure 5.6 shows that the robot started its motion when 10 Newtons of hand contact force is achieved. 0.12 radians of angle have been applied to the wrist angles as a ramp. In addition, change of the inclination angle is also observed during backwards stepping action of the robot in phase six.

When joint angles have reached 0.12 radians for both legs, fifth phase has started. It is a preparation phase to the next phase same as phase three. Since robot will perform a motion in next phase, its required to arrange the force exerted by the robot accordingly. Therefore, the force reference has been increased to 20 Newtons with a ramp as seen in the third phase. The importance of the phase can be analyzed from Figure 5.3. Even 20 Newtons of force is exerted by hands, robot faced with additional hand contact force during performance of one step backwards in a noisy manner. Since, body posture of the robot is changed, environmental interaction forces are affecting the robot's balance in a negative way. That's why 10 Newtons which is applied before leaning against the wall was not enough for the balance of the robot during backward stepping. The increased force value is not the maximum force value that robot can apply to the wall. The value has been determined experimentally with the motivation of obtaining appropriate exerted force to sustain balance of the robot during backwards stepping action happens in phase six.

36

Legs of the robot controlled via position controller with zero moment point base position and reactive feedforward wall force references. Also, control of the arm remains same with the hybrid position-force controller. When the given force, 20 Newtons, is applied to the wall the simulation passed into next phase six. It should be noted that, in this stage force can be increased to a larger value. Actually, it is tested in other simulations and 149 Newtons of wall interaction force is achieved. However, to explore further opportunities to increase force, foot position alteration is studied. Hand contact forces against the force reference can be observed from Figure 5.3. Hand contact force plots a ramp from 10 Newtons to 20 Newtons smoothly same as phase 3.
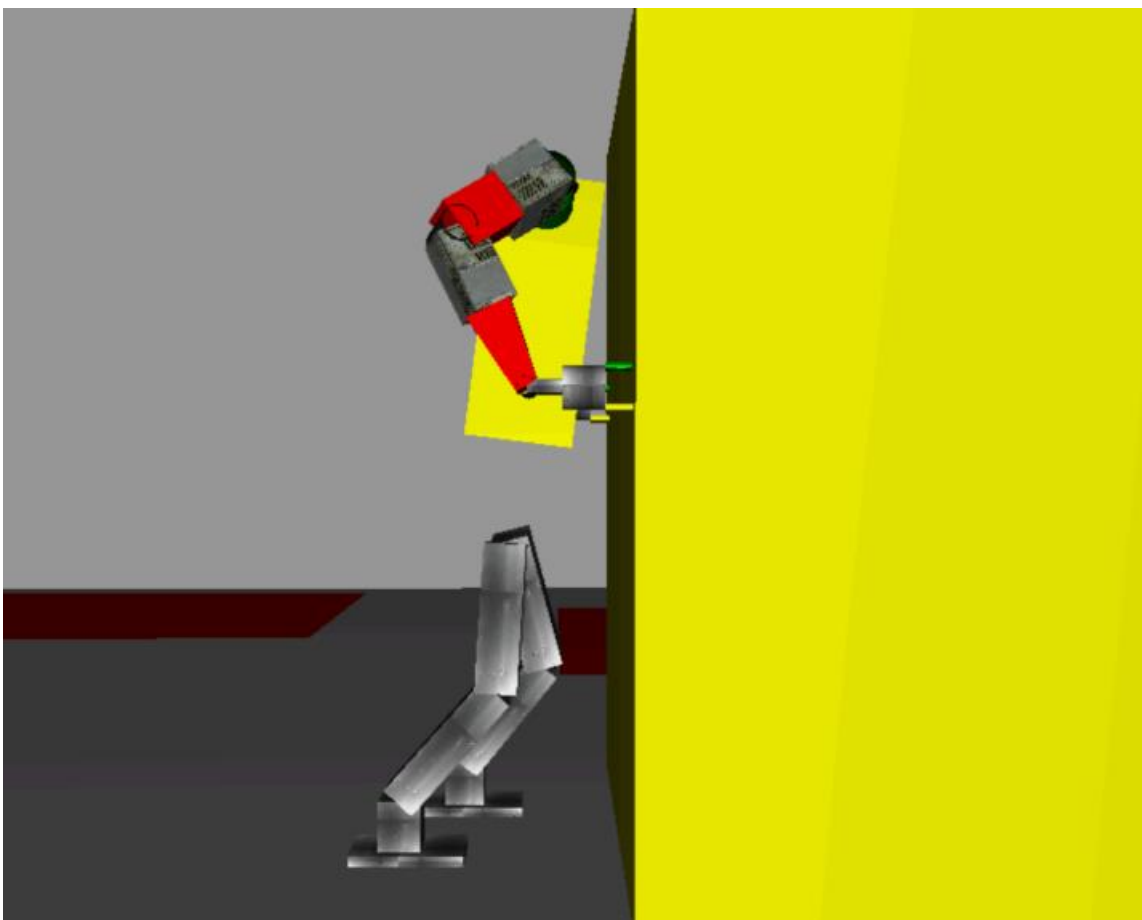
Figure 5.7 The robot performed backward stepping in phase 6

Phase six is the last phase to prepare robot to reach its force exertion limit that this thesis could achieve. In this step, robot performs a backstep to expend its convex hull of the foot supporting area. In this way robot becomes more stable against increased reaction forces due to greater force exertions by the robot. After the backwards stepping has been completed, the simulation is ready to final phase. Motion of the robot can be tracked with Figure 5.8. The robot lifts its foot by 22 centimeters and then put back to the ground after the movement in x axis 13

centimeters backward. Best positions for force exertion are determined experimentally especially for x axis.

Figure 5.8 Position plot of the right foot, which performs backwards stepping, with respect to z-axis (to visualize the amount of lifting) and x-axis (to visualize the size of the step) of world coordinate frame

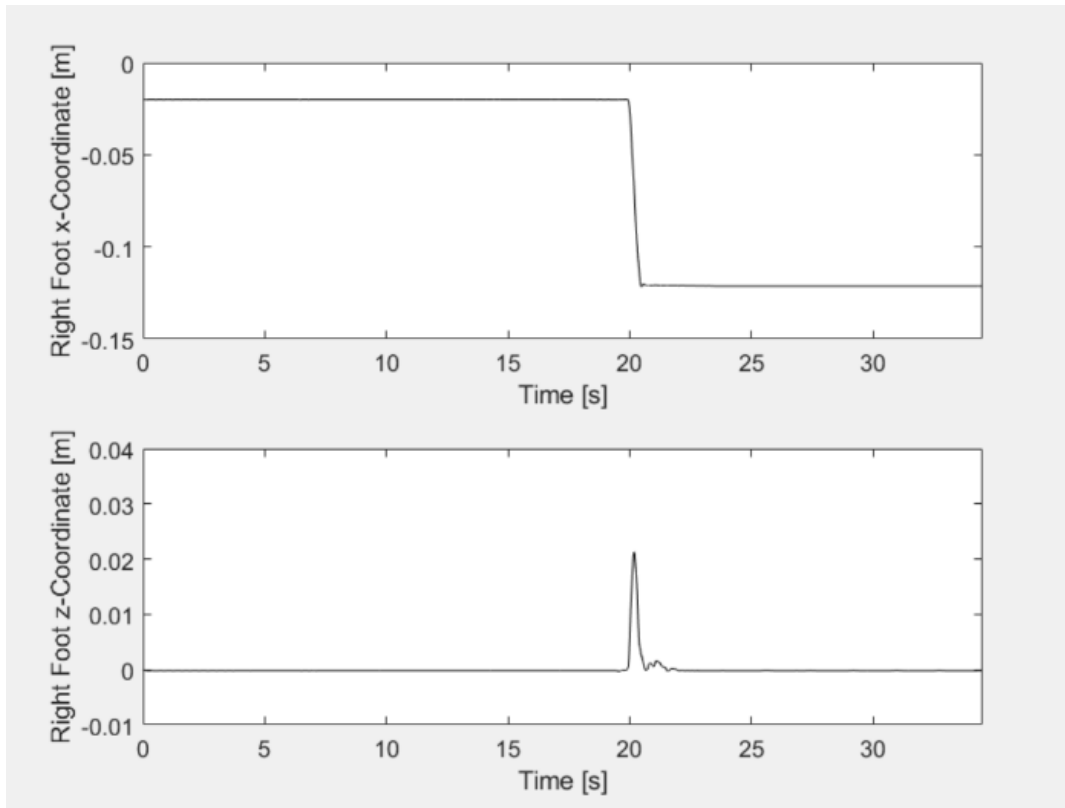In phase seven, the goal is to find our models potential to perform maximum force exertion. In first three phases the foundation of the model has established, ensured that robot has become balanced and modest forces are exerted to test applied control techniques. At phase 4 and phase 6 the amount of force the robot can apply to the wall is increased by changing its posture.

Starting from phase three, reactive feedforward wall force is used as force reference of the legs in conjunction with zero moment point based position reference. The force reference of arm is feedforwarded to leg joint torques after series of operations shown in controller design chapter. This additional toque on the legs caused by the additional force applied by pelvis as known as "pelvis boost". Thus, a simulation model which can perform hybrid arm control, pelvis boost, leaning against the wall, and stepping backwards without losing balance has been established. Owing to these specialties of the application, 183 Newtons of force is exerted to the wall successfully. The force reference is given as a ramp same as previous phases.

6. CONCLUSION

In order to employ humanoid robots as support machines in the human environment a variety of full-body skills are mandatory. Applying force on an immovable surface can be regarded as one such desired motion primitive. This thesis presents a way of motion reference generation and coordination of multiple control schemes for the fulfillment of the pushing task exerting highest force without falling is the most important objective.

Three main tools are employed to reach the goal: i) Pelvis force boost via reactive force planning, ii) introduction of pitch angle for leaning on the wall, iii) stepping backwards in order to enlarge foot support polygon. After the establishment of the first hand contact with the wall, the hand contact reference force is planned carefully in order to keep solid contact which proves to be necessary for the leaning and stepping backwards operations.

Leg and arm control modes, position and force references, their coordination and application timing are developed experimentally and incrementally on a three-dimensional full-dynamics simulation environment developed for the Sabancı University humanoid robot SURALP.

As our simulation studies indicated, the robot can loose and fall backward very easily due to contacting the wall with the hands. The hand contact force which can be reached is a function of the controller, control application timing, body posture and support polygon.

The pelvis force boost tool improves the force applicable on the wall by twenty percent. Leaning on the wall achieves 149 Newtons per hand and stepping back with one foot reaches 183 Newtons.

It can also be deduced from the development and simulation results in this thesis that the maximum contact force attainable can be further improved by extending the parameter range of the forward inclination towards to wall and the size of the foot step made backwards. Employing more than one step is also a natural extension which can be implemented to reach higher hand-wall contact forces without posing the robot fall.

Amount of contact force applied on the wall by hands, in addition being the target of the control scheme in its final stage, is also instrumental to enable leaning and backward stepping phases. It is remarkable that hand contact forces can act as means of balance support for leaning and stepping motion, as well as disturbances which can make the robot fall. The planning and timing of hand contact references is, therefore, of paramount significance.

This thesis work leaves automatic determination of force, inclination angle and backwards step size reference parameters and automatic phase transitions as a future work.

BIBLIOGRAPHY

Akhtaruzzaman, M. and Shafie, A. A. "*Evolution of Humanoid Robot and contribution of various countries in advancing the research and development of the platform*," *ICCAS 2010*, Gyeonggi-do, Korea (South), 2010, pp. 1021-1028, doi: 10.1109/ICCAS.2010.5669646. *and Control*, *102* (2), 69–76.

Aktaş, A. F. (2022). *Full-body motion control of a humanoid robot* (MSc. Thesis)

ASIMOの祖先・兄弟10体が休息する空間｜【Tech総研】. (n.d.). Next.rikunabi.com. Retrieved July 13, 2024, from https://next.rikunabi.com/tech/docs/ct_s03600.jsp?p=001396 Boston: Pearson

Ayhan, O. (2004). *Biped locomotion control via hybrid position control and gravity compensation modes* (Master Thesis).

Ayhan, O. and K. Erbatur, "Biped Walking Robot Hybrid Control with Gravity Compensation," Proc. Int. Conf. on Industrial Electronics, Control and Instrumentation, IECON 2005, Raleigh, USA

Biped Walking Robot. http://www.humanoid.waseda.ac.jp/booklet/kato_4. html (April 8, 2010, 10:00PM)

Capello, S., Moran, M. E., Belarmino, J., Firoozi, F., Kolios, E., & Perrotti, M. (2005). *The da Vinci robot. In 23rd world congress on endourology. J Endourol* (Vol. 19, No. 1, p. A133).

Caron, S., Kheddar, A., & Tempier, O. (2019, May). Stair climbing stabilization of the HRP-4 humanoid robot using whole-body admittance control. In *2019 International conference on robotics and automation (ICRA)* (pp. 277-283). IEEE..

Castano, J. A., Li, Z., Zhou, C., Tsagarakis, N., & Caldwell, D. (2016). Dynamic and reactive walking for humanoid robots based on foot placement control. International Journal of Humanoid Robotics, 13(02), 1550041.

Cheng, G., Hyon, S. H., Morimoto, J., Ude, A., Hale, J. G., Colvin, G., … Jacobsen, S. C. (2007). CB: a humanoid research platform for exploring neuroscience. Advanced Robotics, 21(10), 1097-1114

Chevallereau, C., Bessonnet, G., Abba, G., & Aoustin, Y. (Eds.). (2009). *Kinematic and Dynamic Models for Walking*, (pp. 1–126). John Wiley Sons, Ltd.

Chevallereau, C., Bessonnet, G., Abba, G., & Aoustin, Y. (Eds.). (2013). *Bipedal robots: modeling, design and walking synthesis*. John Wiley & Sons.

Erbatur K., Kurt O., "Natural ZMP Trajectories for Biped Robot Reference Generation," IEEE Transactions on Industrial Electronics, Vol. 56, No. 3, pp. 835-845, March 2009.

Erbatur, K. & Kawamura, A. (2003). A new penalty based contact modeling and dynamics simulation method as applied to biped walking robots. In *Proc. 2003*

Feng, S., Xinjilefu, X., Atkeson, C. G., & Kim, J. (2016, October). Robust dynamic walking using online foot step optimization. In *2016 IEEE/RSJ International Conference on Intelligent Robots and Systems (IROS)* (pp. 5373-5378). IEEE.*FIRA World Congress*, (pp. 1–3).

Fujimoto Y, Kawamura A (1998) Simulation of an autonomous biped walking robot including environmental force Interaction. IEEE Robotics and Automation Magazine, pp 33- 42

Hirai, K. (1999), "The Honda humanoid robot: development and future perspective", Industrial Robot, Vol. 26 No. 4, pp. 260-266. https://doi.org/10.1108/01439919910277431

Hirai, K., Hirose, M., Haikawa, Y., & Takenaka, T. (1998, May). The development of Honda humanoid robot. In *Proceedings. 1998 IEEE international conference on robotics and automation (Cat. No. 98CH36146)* (Vol. 2, pp. 1321-1326). IEEE..

Hirukawa, H. (2007). Walking biped humanoids that perform manual labour. *Philosophical Transactions of the Royal Society A: Mathematical, Physical and Engineering Sciences*, *365* (1850), 65–77.

Hirukawa, H., Kanehiro, F., Kaneko, K., Kajita, S., Fujiwara, K., Kawai, Y., ... & Inoue, H. (2004). Humanoid robotics platforms developed in HRP. *Robotics and Autonomous Systems*, *48*(4), 165-175.

Hyon, S. H., Moren, J., & Cheng, G. (2008, December). Humanoid batting with bipedal balancing. In *Humanoids 2008-8th IEEE-RAS International Conference on Humanoid Robots* (pp. 493-499). IEEE.

Kajita, S., Kanehiro, F., Kaneko, K., Fujiwara, K., Harada, K., Yokoi, K., & Hirukawa, H. (2003, September). Biped walking pattern generation by using preview control of zero-moment point. In *2003 IEEE international conference on robotics and automation (Cat. No. 03CH37422)* (Vol. 2, pp. 1620-1626). IEEE.

Kaneko, K., Harada, K., Kanehiro, F., Miyamori, G., & Akachi, K. (2008, September). Humanoid robot HRP-3. In *2008 IEEE/RSJ International Conference on Intelligent Robots and Systems* (pp. 2471-2478). IEEE.

Kaneko, K., Kaminaga, H., Sakaguchi, T., Kajita, S., Morisawa, M., Kumagai, I., & Kanehiro, F. (2019). Humanoid robot HRP-5P: An electrically actuated humanoid robot with high-power and wide-range joints. IEEE Robotics and Automation Letters, 4(2), 1431-1438.

Kurt, O., & Erbatur, K. (2006, March). Biped robot reference generation with natural ZMP trajectories. In *9th IEEE International Workshop on Advanced Motion Control, 2006.* (pp. 403-410). IEEE.

Kusuda, Y. (2008), "Toyota's violin-playing robot", Industrial Robot, Vol. 35 No. 6, pp. 504-506. https://doi.org/10.1108/01439910810909493

Li L, Xie Z, Luo X, Li J. Trajectory Planning of Flexible Walking for Biped Robots Using Linear Inverted Pendulum Model and Linear Pendulum Model. *Sensors*. 2021

Lim, H.-O. & Takanishi, A. (2000). Waseda biped humanoid robots realizing humanlike motion. In *6th International Workshop on Advanced Motion Control. Proceedings (Cat. No.00TH8494)*, (pp. 525–530)

Lim, H.-o. & Takanishi, A. (2007). Biped walking robots created at Waseda University: WL and WABIAN family. *Philosophical Transactions of the Royal Society A: Mathematical, Physical and Engineering Sciences*, *365* (1850), 49 – 64.

Limited, A. (n.d.). Team HRP2 Tokyo robot during the DARPA Rescue Robot Showdown at Fairplex Fairground June 6, 2015 in Pomona, California. The DARPA event is to challenge teams to design robots that will conduct humanitarian, disaster relief and related operations Stock Photo - Alamy. Www.alamy.com. Retrieved July 13, 2024, from https://www.alamy.com/stock-photo-team-hrp2-tokyo-robot-during-the-darpa-rescue-robot-showdown-at-fairplex-102011276.html

Luh, J. Y. S., Walker, M. W., & Paul, R. P. C. (1980). On-Line Computational Scheme for Mechanical Manipulators. *Journal of Dynamic Systems, Measurement, and Control*, *102* (2), 69–76.

Napoleon, S. Nakaura and M. Sampei, "Balance control analysis of humanoid robot based on ZMP feedback control," *IEEE/RSJ International Conference on Intelligent Robots and Systems*, Lausanne, Switzerland, 2002, pp. 2437-2442 vol.3, doi: 10.1109/IRDS.2002.1041633.

Narang, G., Singh, S., & Narang, A. (2014). Development of a 20 Degrees of Freedom Kid Sized Humanoid Platform with Vision.

Nelson, G., Saunders, A., & Playter, R. (2018). The petman and atlas robots at boston dynamics. *Humanoid robotics: A reference*, 169-186.

Nelson, G., Saunders, A., Neville, N., Swilling, B., Bondaryk, J., Billings, D., Lee, C., Playter, R., & Raibert, M. (2012). PETMAN: A Humanoid Robot for Testing Chemical Protective Clothing. Journal of the Robotics Society of Japan, 30 (4), 372–377

Ogura, Y., Aikawa, H., Shimomura, K., Kondo, H., Morishima, A., Lim, H. O., & Takanishi, A. (2006, May). Development of a new humanoid robot WABIAN-2. In *Proceedings 2006 IEEE International Conference on Robotics and Automation, 2006. ICRA 2006.* (pp. 76-81). IEEE.

Park JH (2003) Fuzzy-Logic Zero-Moment-Point Trajectory Generation for Reduced Trunk Motions of Biped Robots. Fuzzy Sets and Systems, vol 134, no 1, pp 189-203, Elsevier

R. L. Rardin, "Optimization in Operations Research," Prentice Hall , 2000.
Raibert, M., Blankespoor, K., Nelson, G., & Playter, R. (2008). Bigdog, the rough-terrain quadruped robot. *IFAC Proceedings Volumes*, *41*(2), 10822-10825.

Rohan, A., Rabah, M., Nam, K. H., & Kim, S. H. (2018). Design of fuzzy logic based controller for gyroscopic inverted pendulum system. *International Journal of Fuzzy Logic and Intelligent Systems*, *18*(1), 58-64. Scheme for Mechanical Manipulators. *Journal of Dynamic Systems, Measurement,*

Seven U., Akbaş T., Fidan K.C., Erbatur K., "Bipedal robot walking control on inclined planes by fuzzy reference trajectory modification" Soft Computing - A Fusion of Foundations, Methodologies and Applications, vol 500, 2012, Springer Berlin

Seven, U. (2012). *Bipedal humanoid robot control by fuzzy adjustment of the reference walking plane* (Doctoral dissertation).

Shibuya, M.; Sato, T.; Ohnishi, K. Trajectory generation of biped robots using Linear Pendulum Mode with virtual supporting point. In Proceedings of the 10th IEEE International Workshop on Advanced Motion Control, Trento, Italy, 26–28 March 2008; pp. 284–289.

Shibuya, M.; Suzuki, T.; Ohnishi, K. Trajectory Planning of Biped Robot Using Linear Pendulum Mode for Double Support Phase. In Proceedings of the 32nd Annual Conference of IEEE Industrial Electronics, Paris, France, 6–10 November 2006; pp. 4094–4099

Stephens, B. and Atkeson C. G, "Dynamic Balance Force Control for compliant humanoid robots," *2010 IEEE/RSJ International Conference on Intelligent Robots and Systems*, Taipei, Taiwan, 2010, pp. 1248-1255, doi: 10.1109/IROS.2010.5648837.

Taşkıran E, Yılmaz M, Koca Ö, Seven U, Erbatur K (2010) Trajectory Generation with Natural ZMP References for the Biped Walking Robot SURALP. Proceedings of the IEEE International Conference on Robotics and Automation, pp 4237-4242

Taskiran, E., U., Seven, O. Koca, M. Yilmaz and K. Erbatur, "Walking Control of a Biped Robot on an Inclined Plane," Proc. ICONS 2009 - The 2nd International Conference on Intelligent Systems and Control, Istanbul, Turkey, September 2009.

The HRP-3 Promet Mk-II humanoid robot balances its body while... (2007, June 21). Getty Images. https://www.gettyimages.fi/detail/uutiskuva/the-hrp-3-promet-mk-ii-humanoid-robot-balances-its-body-uutiskuva/74843626?adppopup=true

Vukobratović, M., & Borovac, B. (2004). Zero-moment point—thirty five years of its life. *International journal of humanoid robotics*, *1*(01), 157-173.

Vukobratovic, M., Borovac, B., Surla, D., & Stokic, D. (2012). *Biped locomotion: dynamics, stability, control and application* (Vol. 7). Springer Science & Business Media..

WABOT –WAseda roBOT-".http://www.humanoid.waseda.ac.jp/booklet/kato_2. html (April 10, 2010, 12:52AM).

Wikipedia Contributors. (2019, December 1). Leonardo's robot. Wikipedia; Wikimedia Foundation. https://en.wikipedia.org/wiki/Leonardo%27s_robot

Wikipedia Contributors. (2019, November 21). Jaquet-Droz automata. Wikipedia; Wikimedia Foundation. https://en.wikipedia.org/wiki/Jaquet-Droz_automata